Comprehensive Automobile Research System (CARS) – a Python-based Automobile Emissions Inventory Model

Bok H. Baek[1], Rizzieri Pedruzzi[2], Minwoo Park[3], Chi-Tsan Wang[1], Younha Kim[4], Chul-Han Song[5], and Jung-Hun Woo[3,6]

[1]Center for Spatial Information Science and Systems – George Mason University, Fairfax, VA, USA.

[2]Department of Sanitary and Environmental Engineering, Federal University of Minas Gerais, Belo Horizonte, Brazil.

[3]Department of Technology Fusion Engineering, College of Engineering, Konkuk University, Seoul, Republic of Korea

[4]Energy, Climate, and Environment program, International Institute for Applied Systems Analysis, Laxenburg, Austria

[5]School of Earth and Environmental Engineering, Gwangju Institute Science and Technology, Gwangju, Republic of Korea

[6]Civil and Environmental Engineering, College of Engineering, Konkuk University, Seoul, Republic of Korea

corresponding to: Jung-Hun Woo (jwoo@konkuk.ac.kr)

Abstract

The Comprehensive Automobile Research System (CARS) is an open-source python-based automobile emissions inventory model designed to efficiently estimate high quality emissions from motor-vehicle emission sources. It can estimate the criteria air pollutants, greenhouse gases, and air toxins in any spatial resolution based on the spatiotemporal resolutions of input datasets. The CARS is designed to utilize local vehicle activity data, such as vehicle travel distance, road link-level network Geographic Information System (GIS) information, and vehicle-specific average speed by road type, to generate an automobile emissions inventory for policymakers, stakeholders, and the air quality modeling community. The CARS model adopted the European Environment Agency's (EEA) onroad automobile emissions calculation methodologies to estimate the hot exhaust, cold start, and evaporative emissions from onroad automobile sources. It can optionally utilize average speed distribution (ASD) of all road types to reflect more realistic vehicle speed variations. Also, through utilizing high-resolution road GIS data, the CARS can estimate the road link-level emissions to improve the inventory's spatial resolution. When we compared the official 2015 national mobile emissions from Korea's Clean Air Policy Support System (CAPSS) against the ones estimated by the CARS, there is a significant increase in volatile

33 organic compounds (VOCs) (33%) and carbon monoxide (CO) (52%) measured, with a slight
34 increase in fine particulate matter ($PM_{2.5}$) (15%) emissions. Nitrogen oxides (NOx) and sulfur
35 oxides (SOx) measurements are reduced by 24% and 17% respectively in the CARS estimates.
36 The main differences are driven by different vehicle activities and the incorporation of road-
37 specific ASD, which plays a critical role in hot exhaust emission estimates but wasn't implemented
38 in Korea's CAPSS mobile emissions inventory. While 52% of vehicles use gasoline fuel and 35%
39 use diesel, gasoline vehicles only contribute 7.7% of total NOx emissions while diesel vehicles
40 contribute 85.3%. But for VOC emissions, gasoline vehicles contribute 52.1% while diesel
41 vehicles are limited to 23%. Diesel buses comprise of only 0.3% of vehicles and has the largest
42 contribution to NO_x emissions (8.51% of NO_x total) per vehicle due to having longest daily vehicle
43 kilometer travel (VKT). For VOC emissions, Compressed Natural Gas (CNG) buses are the largest
44 contributor at 19.5% of total VOC emissions. For primary $PM_{2.5}$, more than 98.5% is from diesel
45 vehicles. The CARS model's in-depth analysis feature can assist government policymakers and
46 stakeholders in developing the best emission abatement strategies.

47 Keywords: inventory: automobile, vehicle emissions, hot exhaust, cold start, evaporative, python

1 Introduction

49   Globally, ambient pollution causes more than 4.2 million premature deaths every year
50 (Cohen et al., 2017), and Burnett et al. (2018) estimated the health burden is closer to 9 million
51 deaths from ambient PM concentrations. To effectively mitigate air pollutants, governments have
52 been implementing stringent air pollution control policies to reduce harmful regional air pollutants
53 (Hogrefe et al., 2001a; Hogrefe et al., 2001b; Dennis et al., 2010; Rao et al., 2011; Appel et al.,
54 2013; Luo et al., 2019). The chemical transport model (CTM) simulation results strongly rely on
55 precise input data, such as emission inventory, meteorology, land surface parameters, and chemical
56 mechanisms in the atmosphere.

57   The transportation sector is one of the major anthropogenic emissions in urban areas. The
58 tailpipe emissions from the vehicle's combustion process contain many air pollutants, including
59 nitrogen oxides (NOx), volatile organic compounds (VOCs), carbon monoxide (CO), ammonia
60 (NH_3), sulfur dioxide (SO_2), and primary particulate matter (PM) which participates in the
61 formation of detrimental secondary pollutants like ozone and $PM_{2.5}$ in the atmosphere. In the Seoul
62 Metropolitan Area (SMA) in South Korea, transportation automobile sources contribute the most
63 to the total NO_X and primary $PM_{2.5}$ emissions across all emission sources (Choi et al., 2014; Kim
64 et al., 2017a; Kim et al., 2017b; Kim et al., 2017c). Thus, it is critical to understand and better
65 represent the emission patterns from transportation automobile sources in the CTM model. The
66 use of process-based automobile emission models is highly recommended to meet the needs in

67 CTM model because it can estimate high resolution spatiotemporal automobile emissions
68 (Moussiopoulos et al., 2009; Russell and Dennis, 2000).

69   There are two methodologies known in emission inventory development: top-down and
70 bottom-up. The choice of methods is determined by the input data availability. The top-down
71 approach primarily relies on the aggregated and generalized country or regional information, and
72 is typically used in developing countries where only limited datasets and information are available.
73 It has its limitations on representing the vehicle emission process realistically due to the lack of
74 detailed activity and ancillary supporting data. However, the bottom-up approach requires higher
75 quality spatiotemporal activity datasets like road network information, vehicle composition
76 (vehicle type, engine size, vehicle age, and fuel-technology), pollutant-specific emissions factors,
77 road segment length, traffic activity data, and fuel consumption (EEA, 2019; Ibarra-Espinosa et
78 al., 2018b; IEMA, 2017). It can generate more accurate and detailed automobile emissions across
79 various operating processes, such as hot exhaust, evaporative, idling, and hot soak (Nagpure et al.,
80 2016; Ibarra-Espinosa et al., 2018a).

81   There are several bottom-up mobile emissions models available, like MOVES (MOtor
82 Vehicle Emissions Simulator) from the U.S. Environmental Protection Agency (USEPA), the
83 European Environment Agency's (EEA) model COPERT (COmputer Programmed to calculate
84 Emissions from Road Transport), the HERMES (High-Elective Resolution Modelling Emission
85 System) from Barcelona Supercomputing Center (Guevara et al., 2019), the VEIN (Vehicular
86 Emissions INventory) model developed by Ibarra-Espinosa et al. (2017), and the VAPI (Vehicular
87 Air Pollution Inventory) model developed by Nagpure and Gurjar (2012) for India (Nagpure et al.,
88 2016). While these models are all bottom-up emission inventory models, a single model cannot
89 meet all modelers, policymakers, and stakeholders' needs because each model holds its own pros
90 and cons. They are developed differently to meet specific user needs based on the types of traffic
91 activity and emission factors, emission calculation methodologies, and other traffic related inputs
92 such as average speed distribution and geographical resolution. Each model is developed with
93 different levels of specificity, underlying data sets, and modeling assumptions.

94   The MOVES model has the ability to generate high quality emissions for up to 16 different
95 emission processes (i.e., Running Exhaust, Start Exhaust, Evaporative, Refueling, Extended Idling,
96 Brake, Tire, etc.). It can simulate not only county-level but also road segment level emissions
97 depending on data availability. It can also reflect local meteorological conditions, such as ambient
98 temperature and relative humidity, which can significantly impact both pollutants and emissions
99 processes (Choi et al., 2017; Perugu et al., 2018). One major disadvantage of this model is that it
100 is difficult to update and apply to countries outside of the U.S. because it has a high degree of
101 specificity. The COPERT model, widely used in European countries, can model emissions in high
102 resolution, is fully integrated with the EEA's onroad vehicle emissions factors guidelines, and can
103 generate a complete quality assurance (QA) and visualization summary (Ntziachristos et al., 2009).
104 The cons are that it is a proprietary commercial licensed software, limited to EEA guidance, and

105 challenging to modify and update with any key input datasets like the latest emission factors from
106 non-European countries (Lejri et al., 2018; Rey DR, 2021; Li et al., 2019; Lv et al., 2019; Smit et
107 al., 2019).

108   The HERMES and VEIN are both recently released bottom-up inventory models. They
109 have their pros in that they are both open-source models based on open-source computing
110 languages (Python and R), which provide transparency of the emission calculations with a
111 considerable amount of data behind them (Ibarra-Espinosa et al., 2018b; Guevara et al., 2019).
112 Both models are driven by comma-separated value (CSV) formatted input files, making it very
113 easy for users to modify the input datasets. They are also based on the EEA's emission calculation
114 method and equipped with a complete QA and visualization tool based on Python and R libraries.
115 However, it is not an easy task to develop the emission factors, and other required input datasets
116 for other countries and implement any control strategy plan feature to generate a responsive
117 reduced emissions inventory.

118   Overall, there are multiple shortcomings in incorporating these bottom-up models into
119 CTM studies. They require strong programming skills to operate, such as collecting and preparing
120 the input data to fit the model requirements, configuring the model variables, and changing specific
121 variables that may be embedded in the code. Another downside is that while the geographical
122 administration-level (e.g., county level) emissions inventory can be estimated by these models, it
123 requires a 3rd party emissions processor like the SMOKE (Sparse Matrix Operator Kerner
124 Emissions) modeling system (Baek and Seppanen, 2021) to process and generate spatially and
125 temporally resolved emissions inputs for CTM. Some detailed information, like link-level hourly
126 driving patterns, can be lost in the emissions processing steps.

127   There is no single model capable of meeting all the requirements across various spatial and
128 temporal scales (Pinto et al., 2020). However, transparency, simplicity, and a user-friendly
129 interface are requirements for those who mainly work in transportation policy and air quality
130 modeling development (Fallahshorshani et al., 2012; Kaewunruen et al., 2016; Sallis et al., 2016;
131 Sun et al., 2016; Tominaga and Stathopoulos, 2016). Thus, the ideal motor vehicle emissions
132 modeling system would be computationally optimized, easy-to-use, and has a user-friendly
133 interface. Additionally, the model should easily adapt detailed local activity information and the
134 state-of-art emission factors as inputs to represent them in the highest resolution possible
135 temporally and spatially.

136   We have developed the Comprehensive Automobile Research System (CARS) to meet these
137 requirements, especially for the air quality research community, policymakers, and air quality
138 modelers. The CARS is a stand-alone, fully modularized, computationally optimized, python-
139 based automobile emission model. The modularization improves the efficiency of processing times
140 as once district and road link-level annual/monthly/daily total emissions are computed; the rest of
141 the processes are optional. It can generate chemically speciated, spatially gridded, hourly

142 emissions for CTMs without any 3ʳᵈ party programs to develop the highest quality CTM-ready
143 emissions inputs. Details on modularization will be discussed later. The CARS model can be easily
144 adopted and is simple for users to add new functions or modules in the future. The application of
145 the CARS to South Korea will be described in detail later.

2   CARS Emissions Calculation

147   The CARS is an open-source Python-based customizable motor vehicle emissions
148 processor that estimates onroad and offroad emissions for specific criteria and toxic air pollutants.
149 Figure 1 is a schematic of the CARS overview. It applies vehicle, engine, and fuel specific
150 emission factors to traffic data to estimate the local level annual, monthly, and daily total emissions
151 inventory. The emissions inventory calculations require a list of pollutant-specific emissions
152 factors by vehicle age, local activity data, average speed profile/distribution by road type, and
153 geographic information system (GIS) road segment shapefiles inputs. The spatial resolution of
154 vehicle kilometer travel (VKT) determines the CARS geographic scale (i.e. district, county, state,
155 and country) for emission calculations. Unlike the district-level Korea Clean Air Policy Support
156 System (CAPSS) automobile emission inventory (Lee et al., 2011a; Lee et al., 2011b), the CARS
157 applies high resolution annual average daily traffic (AADT) data from the road GIS shapefiles to
158 distribute the total district emissions into road link-level emissions. Optionally, these road link-
159 level emissions can be used to generate spatially gridded CTM-ready emissions input data once
160 the output modeling domain is defined. The summary of input files by categories are presented in
161 Appendix H. How the CARS estimates spatially and temporally enhanced automobile emissions
162 inventories will be discussed in detail next chapter.

163   South Korean traffic databases from the Korea National Institute of Environmental
164 Research (NIER) CAPSS team (Lee et al., 2011b) were used in this study to compute the updated
165 onroad automobile emissions inventory. The databases include individual vehicle activity data
166 (daily total VKT), road activity data (average speed distribution by road), vehicle age specific
167 emission factors, road type information, surface weather data, and GIS road shapefiles.

2.1   Individual Daily Average VKT Activity Data

169   The individual vehicle VKT data is used to reflect human activity. This study imported the
170 national registered vehicle-specific daily total VKT from South Korea's Vehicle Inspection
171 Management System (VIMS), which belongs to the Korea Transportation Safety Authority
172 (KTSA). It contains over 50 million records of vehicle-specific daily total VKT from 2013 to 2017.
173 For the CARS model, we first sorted these records by the vehicle identification number (VIN) to
174 remove any duplicates and then built vehicle-specific daily total VKT traffic activity data in the
175 CSV format. The summary of those vehicle numbers and VKTs is presented in Fig. 2. Sedan
176 vehicles using gasoline fuel comprise the greatest percentage of total vehicles at 47% (~10.4

177   million) and have the highest VKT. While most vehicles demonstrate a paired pattern between the
178   number of vehicles and daily VKT, LPG (liquefied petroleum gas)-fueled taxi shows high VKT
179   with low vehicle numbers due to their long distance travel daily patterns.

180   The VIN (vin) information is used to calculate vehicle-specific daily average VKT (VKT_{vin},
181   km d^{-1}). In Eq. (1), the individual daily average vehicle VKT (VKT_{vin}) is calculated based on the
182   cumulative mileage ($M_{f;vin}$) between the last inspection date ($D_{f;vin}$) and registration date ($D_{0;vin}$).
183   Each vehicle is categorized with Korea's NIER based on a combination of vehicle types (e.g.,
184   sedan, truck, bus, etc), engine sizes (e.g., compact, full size, midsize, etc), and fuel types (e.g.,
185   gasoline, diesel, LPG, etc). Full details of vehicle types and daily total VKT are shown in Appendix
186   A and B.

187
$$VKT_{vin} = \frac{M_{f;vin}}{D_{f;vin} - D_{0;vin}} \qquad (1)$$

188   **2.2   Emission Calculations**

189   Automobile emission sources include motorized engine sources on the paved road network
190   and off the road network (e.g., driveway and parking lots). The CARS model doesn't currently
191   simulate emissions from nonroad emission sources, such as aviation, railways, construction,
192   agricultures, lawn mowers, and boats. The CARS model simulates the onroad automobile
193   emissions from network roads using their local traffic-related datasets. The following section
194   explains the approach of the onroad automobile emission processes. The onroad emission (E_{onroad})
195   in the CARS is defined in Eq. (2), which includes three major emission processes (Ntziachristos
196   and Samaras, 2000):

197
$$E_{onroad} = E_{hot} + E_{cold} + E_{vap} \qquad (2)$$

198   The hot exhaust emissions (E_{hot}) are the vehicle's tailpipe emissions when the internal combustion
199   engine (ICE) combusts the fuel to generate energy under the average operating temperature. The
200   cold start emissions (E_{cold}) are the tailpipe emissions from the ICE when the cold vehicle engine is
201   ignited and the operational temperature is below average condition. The evaporative VOC
202   emissions (E_{vap}) are the emissions evaporated/permeated from the fuel systems (fuel tanks,
203   injection systems, and fuel lines) of vehicles.

204   The CARS first applies the hot exhaust emission factors by vehicle type, age, fuel, engine,
205   and pollutants to individual daily total VKT to compute the hot exhaust emissions. The rest of the
206   processes for cold start and evaporative emissions are calculated afterwards. The emission
207   calculation methodologies used in the CARS model are based on tier 2 and tier 3 methodologies
208   from the EEA's mobile emission inventory guidebook (EEA, 2019) to be consistent with Korea's
209   National Emission Inventory System (NEIS) (Lee et al., 2011a).

2.2.1 Hot Exhaust Emissions

Hot exhaust emissions is the exhaust gas from the combustion process in an ICE. The ICE combustion cycle generally causes incomplete combustion processes which emit hydrocarbons, carbon monoxide (CO), and particulate matter (PM). These are not completely controlled by the after-treatment equipment, such as a three-way catalytic converter, and released into the atmosphere. The sulfur compounds in the fuel are oxidized and become sulfur oxides (SO_x). Nitrogen oxides (NO_x) are produced due to the abundance of nitrogen (N_2) and oxygen (O_2) during the combustion process.

Equation 3 represents the calculation of daily individual vehicle hot exhaust emission rate, $E_{hot; p,vin,myr}$ (g d^{-1}) of pollutant (p). An individual vehicle-specific daily VKT_{vin} (km d^{-1}) is estimated by Eq. (1). The $EF_{hot;p,v,myr,s}$ (g/km) is the hot exhaust emission factor of pollutants (p) for the vehicle type (v), vehicle manufacture year (myr), and average vehicle speed (s). The district's total emission rate is the total hot exhaust emissions from all individual vehicles within the same district.

$$E_{hot; p,vin,myr} = DF_{p,v,myr} \times VKT_{vin} \times EF_{hot; p,v,myr,s} \qquad (3)$$

The deterioration factor (DF) in Eq. (3) is an optional function in the CARS. The deterioration process is caused by vehicle aging and can lead to the increase of vehicle emissions. The vehicle DF is varied by vehicle type (v), pollutant (p), and vehicle manufacture year (myr). The CARS model computes vehicle ages based on the vehicle manufacture year and model simulation year. According to NIER's guidance on calculating deterioration factors, there is no deterioration in a new vehicle during their first five years. After five years, the deterioration factors can range from 5% to 10% depending on the type of vehicle and pollutants. Deterioration processes can cause up to an 100% increase of emissions in fifteen-year-old vehicles. Currently, the DF is an empirical coefficient that varies by vehicle age (Lee et al., 2011a).

The hot exhaust emission factor, $EF_{hot;p,v,s}$ (g/km) is a function of vehicle speed (s) with other empirical coefficients: a, b, c, d, f, k. The emission factor formula and those coefficients were developed by NIER's CAPSS (Lee et al., 2011a). These coefficients are varied by pollutants (p), vehicle type (v), vehicle manufacture year (myr), and vehicle speed (s). The vehicle speed affects the combustion efficiency of an ICE and impacts the emission rates and its composition from the tailpipe.

$$EF_{hot; p,v,myr,s} = k(a \times s^b + c \times s^d + f) \qquad (4)$$

While vehicle speed plays a critical role in hot exhaust emissions from most vehicles, NOx emissions from some diesel vehicles show sensitivity to local ambient temperature and humidity due to the atmospheric moisture suppression of high combustion temperatures that lower NO_x emissions at higher humidity (Choi et al., 2017; Ntziachristos and Samaras, 2000). Figure 3 shows

244   the dependency of NO_x emission factors from compact diesel vehicles to vehicle speed (Fig. 3a)
245   and ambient temperature (Fig. 3b). Figure 3a shows a significant decrease of NO_x emissions when
246   the speed increases between 0 and 70 km. Figure 3b demonstrates the significance of local
247   meteorology on NO_x emissions from a compact diesel sedan. Based on these NIER's CAPSS
248   emission factors, the sensitivity to local ambient temperature is limited to NO_x pollutant emissions
249   from diesel vehicles.

250   Due to its high sensitivity to the vehicle operating speed, it is important for the CARS to
251   simulate realistic speed patterns for accurate emissions estimates. When a single speed is assigned
252   to compute hot exhaust emissions, it won't reflect the emissions under low-speed circumstances.
253   To overcome this limitation, the CARS has adopted the 16 average speed bins concepts for a better
254   representation of vehicle speed distribution that varies by road type (i.e., local, highway,
255   expressway). We have implemented a feature for the CARS optionally to apply road-specific
256   average speed distributions (ASD) ($A_{bin,r}$) by 16 speed bins (*bin*) (from 0 to 121 km h^{-1} defined in
257   Appendix E) for eight different road types (*r*) (No.101-108, shown in Appendix C) as classified
258   by CAPSS (Fig. 4a). Although ASD patterns vary by region and time, the current CARS model
259   version does not support ASD application by region and time of day due to the lack its availability
260   in South Korea.

261   We first developed the ASD (Fig. 4a) for eight different road types (No. 101-108) in South
262   Korea based on the latest road link-specific average speed and the length of link from the SK GIS
263   road network shapefiles (NIER, 2018). However, the ASD based on the SK GIS road shapefiles
264   did not capture low speed (<16 km h^{-1}) driving (Fig. 4a). This causes a significantly lower
265   estimation of NOx and VOC emissions compared to the CAPSS (Appendix G). We believe the
266   SK average speed distribution is missing low speed driving that can occur due to traffic congestion.
267   To address this absence of low-speed driving in the SK ASD, we incorporated data from the ASD
268   (Figure 4b) from the state of Georgia to the low speed ranges (speed bin #1 and #2 for road type 1
269   to 7). We increased the total fractions of low speed bins (the 2:1 ratio of fractions of bin #1 and
270   #2) by 2% for interstate expressways, 3% for urban expressways, 7% for all highways, and 15%
271   for all local roads. The increases in low speed bins lowered the distributions of other higher speed
272   bins homogeneously due to the renormalization of fractions by road type. Figure 4c shows the
273   renormalized hybrid-ASDs of all road types based on SK ASD and Georgia ASD. We understand
274   that the hybrid-ASD approach is not ideal for SK onroad emission inventory development, but it
275   clearly demonstrates the CARS's capability and sensitivity to the vehicle speed representation.

276   While 16 speed bins ASD application is critical to computing more realistic hot exhaust
277   emissions, there should be some restrictions on certain road types. Users can adjust the restricted
278   roads control table input file to limit the vehicle types that are only operated on a particular road
279   type. For example, motorcycles are limited to local roads (No. 104, 106, and 107), but not on
280   expressways (No. 101, 102, 103, 105, and 108) due to its traffic regulation rules. Heavy trucks are
281   only allowed on the highway (No. 101, 102, 103, 105, and 108.) by law. The details of the road

282 restriction control table format can be found on the CARS's user's guide from the CARS version
283 1 used in this paper (Baek et al., 2021).

284 The 16 speed bins ASD from Eq. (13) are added to the CARS hot exhaust emissions
285 equation (Eq. 3). The hot exhaust emissions from individual vehicles ($E_{hot;p,vin,myr}$) can be
286 calculated by considering road-specific speed bins distribution (Eq. 5). Although the vehicles may
287 be operated in different districts from their registered district, this is our best method to estimate
288 the vehicle speed for hot exhaust emissions.

289 $$E_{hot; p,vin,myr} = DF_{p,v,myr} \times \sum_{bin}(VKT_{vin} \times EF_{hot; p,v,myr,s} \times A_{bin,r}) \qquad (5)$$

290 **2.2.2 Cold Start Emissions**

291 The cold start emissions occur when a cold engine vehicle is ignited. Lower temperatures
292 of the ICE are not optimal conditions for complete fuel combustion. This process lowers the
293 combustion efficiency (CE) and increases the emissions of hydrocarbon and CO pollutants from
294 the tailpipe exhaust (Jang et al., 2007). The CARS can estimate the cold start emissions for vehicles
295 using gasoline, diesel, or liquefied petroleum gas (LPG) fuel. Besides the vehicle and engine type,
296 road type also plays a critical role in the quantity of cold start emissions because it occurs mostly
297 in parking lots and rarely on highways.

298 The cold start emission, E_{cold} (g d^{-1}), is derived from the hot exhaust emissions, the ratio of
299 hot to cold exhaust emissions (EF_{cold}/EF_{hot} -1.0), and the percentage of the traveled distance with
300 a cold engine (Eq. 6).

301 $$E_{cold; p,v} = \beta_T \times E_{hot; p,v} \times \left(\frac{EF_{cold; p,v}}{EF_{hot; p,v}} - 1.0\right) \qquad (6)$$

302 The emission factor of cold start emissions (EF_{cold}) is not directly calculated from
303 measurement data like hot exhaust emissions ($E_{hot;p,v}$), but measured under different ambient
304 temperatures (*T*). The CARS model applies linear regression models developed by CAPSS to
305 estimate the increasing ratio of cold start to hot exhaust emissions (EF_{cold}/EF_{hot}) under different
306 temperatures (*T*) (Eq. 7). In this equation, *A* and *B* are the empirical coefficients that vary by the
307 pollutants (*p*) and vehicle type (*v*).

308 $$(\frac{EF_{cold; p,v}}{EF_{hot; p,v}}) = A_{p,v} + B_{p,v} \times T \qquad (7)$$

309 β is the percentage of the distance traveled under a cold engine and also depends on the
310 ambient temperature. Cold ambient temperatures cause a longer distance traveled under a cold
311 engine due to the slower heating time. According to the CAPSS database for Seoul city (Lee et al.,
312 2011a), the empirical linear equation for β is shown in Eq. (8). This formula represents how

313   ambient temperature affects β. For example, when the average temperature is -2°C, β is 34.8%. In
314   summer, the monthly average temperature is 25.7°C, which causes β to drop to 21%.

315 $$\beta = 0.647 - 0.025 \times 12.35 - (0.00974 - 0.000385 \times 12.35) \times T \qquad (8)$$

316   **2.2.3   Evaporative VOC Emissions**

317   Evaporative emissions are emissions from vehicle fuel that are evaporated into the
318   atmosphere. This occurs in the fueling system inside the vehicle, such as fuel-tanks, injection
319   systems, and fuel lines. Diesel vehicles, however, can be exempted due to diesel fuel's low vapor
320   pressure. The primary sources of evaporative emissions are breathing losses through tank vents
321   and fuel permeation/leakage. The CARS model adopted the EEA's emission inventory guidebook
322   (EEA, 2019) to account for diurnal emissions from the tank (e_d), hot and warm soak emissions by
323   fuel injection type (S_{fi}), and running loss emissions (R) (Eq. 9). Unlike CAPSS, there is a
324   conversion factor (0.075) applied to E_{vap} for motorcycles to prevent an overestimation of VOC.

325 $$E_{vap;\,p,v} = \left(e_{d;\,p,v} + S_{fi;\,p,v} + R_{l;\,p,v}\right) \qquad (9)$$

326   Diurnal emissions, e_d (g d^{-1}), during the daytime are caused by the ambient temperature
327   increase and the expansion of fuel vapors inside the fuel tank. Most of the current fuel tank systems
328   have emission control systems to limit this kind of evaporative VOC emissions. The e_d can be
329   calculated with the empirical Eq. (10), which was developed by CAPSS. T_l is the monthly average
330   of the daily lowest temperatures and T_h is the monthly average of the daily highest temperatures.
331   The empirical coefficient α is 0.2, which represents how 80% of emissions are eliminated by the
332   vehicle emission control system.

333 $$e_d = \alpha \times 9.1 exp[0.3286 + 0.0574 \times (T_l) + 0.0614 \times (T_h - T_l - 11.7)] \,(10)$$

334   Soak emissions (S_{fi}) occur when a hot ICE is turned off; the remaining heat from the ICE
335   can increase the fuel temperature in the system which causes the increase of evaporative VOC
336   emissions. This carburetor float bowls are the major source of the soak emissions. Newer vehicles
337   with fuel injection and returnless fuel systems do not emit soak emissions. Because most of the
338   current vehicles in South Korea have a new fuel system, soak emissions (S_{fi}) in the CARS model
339   are set to 0.

340   The running loss emissions (R_l) are from vapors generated in the fuel tank when a vehicle
341   is in operation (Eq. 11). In some older vehicles, the carburetor and engine operation can increase
342   the temperature in the fuel tank and carburetor, which can cause a significant increase in
343   evaporative VOC emissions. VOC emissions from running loss can be greatly increased during
344   warmer weather. However, newer vehicles with fuel injection and returnless fuel systems are not

345 affected by the ambient temperature. Because most vehicles in South Korea do not use carburetor
346 technology, we expect running loss emissions to have the least impact (Lee et al., 2011b).

$$347 \qquad R_l = \alpha \times L_{r,v} \times [(1 - \beta) \times R_h + \beta \times R_w] \qquad (11)$$

348   The empirical coefficient α is 0.1 here, which represents that 90% of the running loss is
349 avoided by the newer fuel system. L is the distance traveled (km) by road and is the same one used
350 in hot exhaust emission calculations. β is the same parameter from Eq. (8). The R_h and R_w are the
351 average emission factors from running loss under hot and warm/cold conditions, respectively.

352   2.3   Road Link-Level Emissions Calculations

353   In general, district-level automobile emissions calculations are driven by district-level
354 averaged vehicle activity and operating data, which do not reflect realistic spatial patterns of
355 onroad automobile emissions. The CARS model introduces road link-specific traffic data by
356 default to develop spatially enhanced road link-specific emissions that are more representative of
357 the emissions. This high-resolution traffic data is a GIS shapefile that is composed of many
358 connected segments, which are called "road links." All road links hold information such as
359 start/end location coordinates, AADT, road link length, averaged vehicle speed, and road type (No.
360 101-108).

361   The CARS model applies link-level AADT ($AADT_{d,r,l}$, d^{-1}) and road length ($L_{d,r,l}$) to
362 compute the road link-specific VKT ($VKT_{d,r,l}$, km d^{-1}) in Eq. (12). The road links are identified by
363 district (d), road type (r), and link (l) labels. The road VKT is a parameter that reflects the traffic
364 activity of each road link and it is different from individual daily vehicle activity data ($VKT_{v,age}$)
365 in Eq. (1).

$$366 \qquad VKT_{d,r,l} = AADT_{d,r,l} \times L_{d,r,l} \qquad (12)$$

367   Road link-specific VKT ($VKT_{d,r,l}$) is used to redistribute the district total emissions (E_{onroad})
368 from Eq. 2 into road link-level emissions. The following three weight factors are computed: the
369 district weight factors, ω_d (Eq. 13), the road type weight factors, $\omega_{d,r}$ (Eq. 14), and the road-link
370 weight factors, $\omega_{d,l}$ (Eq. 15). The weight district factors (ω_d) are the renormalization of each
371 district's total VKT over state-level total VKT (N is the number of districts). The main reason we
372 performed the renormalization over state-level total VKT is to reflect daily traffic patterns from
373 multiple districts under the assumption that most vehicles travel within the same state. The road
374 type weight factors by district ($\omega_{r,d}$) are used to compute road-specific emissions, while road-
375 specific averaged speed distributions (ASD; $A_{s,r}$) from Eq. (5) are applied to capture vehicle
376 operating speeds by road type. The road link weight factors ($\omega_{d,l}$) are then applied to redistribute
377 the district emissions into road link-level emissions.

378

$$\omega_d = \frac{\sum_r \sum_l VKT_{d,r,l}}{\frac{1}{N} \sum_d \sum_r \sum_l VKT_{d,r,l}} \qquad (13)$$

379

$$\omega_{d,r} = \frac{\sum_l VKT_{d,r,l}}{\sum_r \sum_l VKT_{d,r,l}} \qquad (14)$$

380

$$\omega_{d,l} = \frac{VKT_{d,r,l}}{\sum_r \sum_l VKT_{d,r,l}} \qquad (15)$$

381

3 CARS Configuration

382

383   The CARS model is an open-source program based on Python (Guido van Rossum, 2009)
384   that allows the users to efficiently apply open-source modules to develop programs. Users can
385   easily install Python development tools and load customized packages and modules to set up the
386   CARS development environment. All CARS modules are developed using Python v3.6. Other than
387   the GIS road shapefiles, all input files are based in the ASCII CSV format, which can be easily
388   handled by both spreadsheet programs and programming languages, making it more accessible for
389   users of all skillsets. The CARS can not only estimate district-level and spatially enhanced road
390   link-level emissions, but can also generate hourly chemically speciated gridded emissions for
391   CTMs. In addition, the CARS also generates various summary reports, graphics, and
392   georeferenced plots for quality assurance.

393   The required Python modules for the CARS are: "***geopandas,***" "***shapely.geometry***", and
394   "***csv***" modules to read the shapefiles and table data files. The "***NumPy***" and "***pandas***" modules
395   are used to operate the memory arrays and scientific calculations, while the "***pyproj***" module deals
396   with converting the projection coordinate systems. "***matplotlib***" is for generating any type of
397   figures/plots. Furthermore, the CARS model can also read and write Climate and Forecast (CF)-
398   compliant NetCDF-formatted files using "***NetCDF4***".

399   The first process in the CARS is "***Loading_function_path***"; it allows users to define and
400   check the input file paths. Once all input files are checked, there are six process modules in CARS
401   to process inputs, compute emissions, and generate various output files, including QA reports.
402   Figure 5 is the schematic of the CARS that consists of six process modules with various functions.
403   The six process modules are (1) "**Process activity data**", (2) "**Process emission factors**", (3)
404   "**Process shapefile**, (4) "**Calculate district emissions**", (5) "**Grid4AQM**", and (6) "**Plot figures**".
405   The main purpose of modularizing the CARS is to meet the needs of various communities, such
406   as policymakers, stakeholders, and air quality modelers. While modules (1) through (4) are
407   required to develop the district-level and road link-level emissions inventories, module (5)
408   "**Grid4AQM**" is optional depending on if users want to develop chemically-speciated gridded
409   hourly emissions for CTMs. Also, the modularity of the CARS allows users to bypass certain

410   modules if it has been previously processed without any changes. For example, if there is no
411   change in traffic activity, emission factors table, or GIS shapefiles, users do not need to run these
412   modules and can simply read the data frame outputs and then run "**Grid4AQM**" for the modeling
413   dates and domain. The "**Grid4AQM**" module will not only improve the computational time for
414   CTMs but also eliminate the need for a 3rd party emissions modeling system like SMOKE (Baek
415   and Seppanen, 2021).

416   The rectangle boxes in Fig. 5 represent the data array and the boxes with rounded edges are
417   the functions in the CARS. Details on the CARS code, input table format, and functions setup
418   information can be found on the CARS GitHub website (Pedruzzi *et al*., 2020).

419   The "**Process activity data**" module first reads the vehicle activity data, such as an
420   individual vehicle's daily total VKT based on its registered district. The "**Process emission factors**"
421   module reads and stores the emission factors table that holds all pollutant emission factors to
422   estimate the emissions for all vehicles. Meteorology-sensitive emission factors are only limited to
423   NO_x pollutants. District boundary GIS shapefiles and road network shapefiles are processed
424   through "**Process shape file**" to generate the VKT-based redistribution weighting factors from Eq.
425   (13), (14) and (15) for the "**Calculate district emissions**" module to compute district-level and
426   road link-level emission rates (metric tons per year, $t\ yr^{-1}$).

427   The redistributed emission rates ($t\ yr^{-1}$) from the "**Calculate district emissions**" module
428   present annual total emission rates until district-level VKTs from the "**Process activity data**"
429   module are added. Then, the "**Grid4AQM**" module can generate CTM-ready chemically speciated
430   emissions. The "***Read_chemical***" function from the "**Grid4AQM**" module is designed to process
431   the chemical speciation profile that can convert the inventory pollutants such as CO, NO_X, SO_2,
432   PM_{10}, $PM_{2.5}$, VOC, and NH_3, into the chemically lumped model species that CTM requires for
433   chemical mechanisms, such as SAPRC (L. and Heo, 2012) and Carbon Bond version 6 (CB6)
434   (Yarwood and Jung, 2010). The "***Read_temporal***" function processes the complete set of monthly,
435   weekly, and hourly temporal allocation profiles that can convert annual total emissions to hourly
436   emissions. "***Read_griddesc***" defines the CTM-ready modeling domain and computes the gridding
437   fractions for all road link-level emissions by overlaying the modeling domain over the GIS
438   shapefiles. Once annual total emissions are chemically speciated, spatially gridded, and temporally
439   allocated into hourly emissions, the "***Gridded_emis***" function will combine emission source-level
440   conversion fractions from each function (***Read_chemical***, ***Read_temporal***, and ***Read_griddesc***) to
441   generate the CTM-ready chemically speciated, gridded hourly emissions in the NetCDF binary
442   format. The "**Plot Figures**" module is designed for generating various summary reports and
443   graphics to assist users in understanding the estimated automobile emissions inventory computed
444   by the CARS. The following section will describe the detailed processes of the "**Grid4AQM**"
445   module, which includes chemical, spatial, and temporal allocations.

446   The influence of temperature on emission processes are considered in the CARS model.
447   There are three temperature parameters in current CARS model such as "temp_max" for maximum
448   temperature, "temp_mean" for mean temperature, and "temp_min" for minimum temperature.
449   These temperature parameters will be applied to over the entire modeling domain during the
450   simulation period. Current CARS model version does not support to process gridded meteorology
451   data from the 3rd party meteorology models like Meteorology-Chemistry Interface Processor
452   (MCIP) from U.S. EPA., and Weather Research Forecasting (WRF) model from National Center
453   for Atmospheric Research (NCAR) yet. However, CARS can easily adopt various temporally
454   resolved temperature values by adjusting the CARS simulation period (i.e., day, week, month,
455   season, or annual).

3.1   Chemical Speciation

457   To support CTMs applications, the CARS needs to be able to convert inventory pollutants
458   into chemical lumped model species based on the choice of CTM chemical mechanisms. NO_x
459   includes nitric oxide (NO), nitrogen dioxide (NO_2), and nitrous acid (HONO). VOCs can represent
460   hundreds of different organic carbon species, such as benzene, acetaldehyde, and formaldehyde.
461   These grouped inventory pollutants cannot be directly imported into the chemical mechanism
462   modules in the CTM system and require chemical speciation allocation for CTMs to process them
463   during their chemical reactions. Therefore, the "**Grid4AQM**" module performs the chemical
464   species allocation step prior to the temporal and spatial allocations to generate the gridded hourly
465   emissions. The "***Read_chemical***" function in "**Grid4AQM**" module allows users to assign these
466   emission inventory pollutants to CTM-ready surrogate chemical species (a.k.a lumped chemical
467   species) by vehicle, engine, and fuel type. For example, VOC emissions from diesel busses can be
468   converted into the following composition based on its chemical allocation profile: alkanes (68%),
469   toluene (9%), xylenes (8%), alkenes (4%), ethylene (2%), benzene (1.3%), and unreactive
470   compounds (7%) when the CB6 chemical mechanism is selected. Further details on the chemical
471   speciation profile input formats are available in the CARS user's guide.

3.2   Spatial Allocation

473   The "**Calculate district emissions**" module calculates both total district and road link
474   specific emissions based on road link-specific AADT data from road network GIS shapefiles. The
475   "**Calculate district emissions**" module first gets the district total vehicle emissions (Eq. 2) based
476   on the district-level VKTs, and then the normalized district total emissions by district weight factor,
477   ω_d (Eq. 13). Afterwards, the normalized district total emissions are redistributed into every road
478   link using road link-level weight factors ($\omega_{d,l}$) (Eq. 15). The district total emissions from Eq. (2)
479   and from Eq. (15) remain the same. Then the computed road link-level emissions then will be

480   converted into grid cell emissions using the modeling domain grid cell fractions computed in the
481   "***Read_griddesc***" function in the "**Grid4AQM**" module.

3.3   Temporal Allocation

483   Once chemical and spatial allocations are completed, the final step to support CTM
484   application is a temporal allocation that converts the annual total emissions from the "**Calculate**
485   **district emissions"** module into hourly emissions. The "***Read_temporal***" temporal allocation
486   function in the "**Grid4AQM"** module converts the annual emission rate (t yr^{-1}) to the hourly
487   emission rate (mol hr^{-1}) using monthly, weekly, and weekday/weekend diurnal temporal profiles.
488   This module processes these temporal profile inputs, which are the monthly (January - December),
489   weekly (Monday - Sunday), and weekday/weekend 24-hour profile tables (0:00-23:00 LST). The
490   users can assign these temporal profiles with a combination of vehicle, engine, fuel, and road types
491   to enhance their temporal representations in detail.

3.4   Chemical Transport Model Emissions

493   The main goal of the **"Grid4AQM"** module is to generate temporally, chemically, and
494   spatially enhanced CTM-ready gridded hourly emissions. First, it reads the CTM modeling domain
495   configuration and then overlays it over the road network GIS shapefile and district-boundary
496   shapefile to define the modeling domain. This overlaying process between the road network,
497   district boundary GIS shapefiles, and modeling domain allows the **"Grid4AQM"** module to
498   compute the fraction of road links that intersects with each grid cell. Figure 6 demonstrates how
499   the district boundary and road network GIS shapefiles are used to perform the spatial allocation
500   processes in CARS. Figure 6a is a native road link shapefile of Seoul with AADT, VKT, district
501   ID, and road type. Figure 6b presents an overlay of two districts' road links (purple and blue) over
502   the selected region. State total emissions will be renormalized into weighed district total emission
503   data and then redistributed into the road link. Figure 6c illustrates how the weighted road link-
504   level emissions get allocated into modeling grid cells for CTMs. The link-level VKT ($VKT_{d,r,l}$)
505   from Eq. (12) will be used to compute a total of traffic activity fractions by grid cell and then use
506   that to assign the link-level emissions from Eq. (2) into each grid cell. When a road link intersects
507   with multiple grid cells, the "**Grid4AQM"** module will weigh the emissions by the length of the
508   link that intersects with each grid cell. It should be noted that current CARS model can only
509   generate the Community Multiscale Air Quality (CAMQ)-ready gridded hourly emissions in
510   format of IOAPI (Input/Output Applications Programming Interface) based on NetCDF format.

511   Through the overlay process, the CARS model can generate various types of output data,
512   such as total district emissions, link-level emissions, and CTM-ready gridded emissions. For
513   example, the CO vehicle emissions from the Seoul metropolitan in South Korea are presented in
514   three different output formats in Fig. 7. Figure 7a shows the annual mobile $PM_{2.5}$ emissions by

515   district. The road link level annual emissions are presented in Fig. 7b. Furthermore, the CARS
516   applies the link-level emissions from Fig. 7b to generate the hourly grid cell emission data with a
517   1 km × 1 km resolution for the CTM in Fig. 7c.

518   **3.5   National Control Strategy Application**

519   One of the unique features in the CARS compared to other mobile emissions models is that
520   it can promptly develop a strategy to control automobile emissions in response to   national
521   emergency high $PM_{2.5}$ episodes. It is very common to experience high $PM_{2.5}$ episodes, especially
522   during the wintertime in South Korea due to domestic and international primary and secondary air
523   pollutants emissions. When the 72-hour forecasted $PM_{2.5}$ concentration exceeds the average 50
524    $\mu g/m^3$ (0:00-16:00 LST), the national $PM_{2.5}$ emergency control strategy is activated for ten days.
525   It applies a nationwide vehicle restriction policy within 24 hours. It enforces a limit on what kind
526   of vehicles can be operated on a certain date. The restrictions can be closures of public parks and
527   government facilities and of certain vehicles based on their fuel type and age, which is a major
528   factor of engine deterioration. This policy will limit the number of vehicles on the network roads
529   significantly, which could reduce primary $PM_{2.5}$ and precursor pollutant (NOx, NH_3, and VOC)
530   emissions, especially from heavily populated metropolitan regions (Choi et al., 2014; Kim et al.,
531   2017a; Kim et al., 2017b; Kim et al., 2017c).
532   To understand the impacts of an even or odd vehicle number restriction policy in real-time,
533   we need to quickly develop a rapid controlled response emissions for the air quality forecast
534   modeling system based on the reduced number of vehicles on the road. The process of generating
535   the controlled mobile emission inventory can take a long time if we start fresh. Thus, we have
536   implemented this control strategy as an optional "*Control Factors*" function in the "**Calculate**
537   **district emissions**" in the module for users to quickly and easily generate the controlled mobile
538   emission inventory with consideration of the limited number of vehicles based on the vehicle,
539   engine, fuel, and vehicle manufactured year. A one hundred percent (100%) control factor means
540   that there are no emissions from those selected vehicles.

541   Because of the modularization system in the CARS, we can bypass some computationally
542   expensive data processing modules (i.e., "**Process activity data**", "**Process emission factors**",
543   and "**Process shape file**") and let the "**Calculate district emissions**" module quickly apply control
544   factors while it computes the district-level mobile emission inventory from Eq. (2). This will allow
545   users to reduce the computational time to generate the controlled mobile emissions under a specific
546   control scenario and develop the controlled CTM-ready gridded hourly emissions using the
547   "**Grid4AQM**" module.

3.6   Computational Time

While the CARS can generate a high-quality spatiotemporal emission inventory, it is quite critical for the CARS to generate them effectively and accurately without being at the expense of computational time. This is especially important to meet the needs for an air quality forecast modeling system responding to a national emergency control strategy implementation.

In this section, we will discuss the details of the CARS computational modeling performance. While the CARS model has been highly optimized, the modularization of CARS has also improved its modeling performance with its optional module runs. The breakdown of module specific computational time estimates based on the benchmark CARS runs are listed in Table 1. The benchmark CARS case includes a total of 24,383,578 daily VKT datasets from KSTA over two different years, 84,608 emission factors for all pollutants across a combination of vehicle-age-engine-fuel types, 385,795 road links from the GIS road network shapefiles, 5,150 districts/16-states boundary GIS shapefile, and 5,494 grid cells (=82 rows and 67 columns) for CTMs. Without any computational parallelization, the total processing time of all six modules usually takes around a half hour to generate a single day CTM-ready gridded hourly emission file. However, it can be further shortened to 25-30 minutes on a higher performance computer. Because of the modular system implemented in the CARS, generating one month (31 days) long gridded hourly emissions from CTMs in 100 minutes on high-performance computers. The maximum usage of RAM can reach up to 11 GB. Table 1 shows the breakdown of computational time by each module from two different hardwares (desktop and laptop computers). The numbers in parentheses beside the **"Grid4AQM"** module is the computational time for a single day versus 31 days. While the **"Grid4AQM"** module takes an average of 4.9 minutes for a single day emissions generation, processing a consecutive 31 days saves 46% more time, decreasing it from 151.9 minutes (=4.9 minutes * 31 days) to 81.6 minutes.

4   Results

CARS and CAPSS Comparison

The CARS model calculates the 2015 onroad automobile emissions based on the latest 2015 emission factors and the 2015-2017 vehicle activity database in South Korea. The annual total emissions from CARS are compared against the ones from NIER's CAPSS in Table 2. The CARS model estimated the following annual total emissions in units of metric tons per year (t yr^{-1}): NO$_x$ (301,794); VOC (61,186); CO (373,864), NH$_3$ (12,453); PM$_{2.5}$ (10,108), and SO$_x$ (172.0). Compared to NIER's CAPSS, the CARS underestimated NO$_x$ (-18% decrease) and SO$_x$ (-17% decrease), and overestimated the emissions of VOC by 33%, PM$_{2.5}$ by 15%, CO by 52%, and NH$_3$ by 24%. Both NIER's CAPSS and CARS shared the same emission factor tables, which hold over

582   84,608 emission factors for all pollutants across a combination of vehicle, age, engine, and fuel
583   types.

584   The difference in results between CAPSS and CARS are caused by three following reasons.
585   First, the number of vehicles used in CARS is slightly higher (6%) than CAPSS data (1.3 out of
586   23 million), as well as other key traffic-related activity inputs (i.e., vehicle age distribution,
587   averaged speed distribution, etc). Secondly, the vehicle speed information assigned by vehicle and
588   road type play a critical role. The CAPSS calculation was based on the road-specific a signle
589   average speed value or 80% of the speed limit of the road as an input of vehicle operating speed
590   for three road types (rural, urban, and expressway) (Lee et al., 2011b). In other words, CAPSS
591   only assigns a "single-speed value" for each road type, and does not encounter the variation of
592   vehicle speed during its operation on roads into the emissions calculation. Most running exhaust
593   emissions occur during a vehicle's low-speed operation due to its incomplete combustion of fuel,
594   and it is critical to accurately represent the emissions across various speed bins in order to compute
595   the accurate emissions (Fig. 4). A detailed analysis of the impact of vehicle speed will be discussed
596   later in this chapter. Lastly, other advanced processes in the CARS, such as link-level AADT and
597   district-level vehicle data (5,150 districts in South Korea) can reflect more spatial detail and
598   variation than the CAPSS. The CAPSS only considers state-level data (17 states in South Korea)
599   and five road types (interstate expressway, urban highway, rural highway, urban local, and rural
600   local).

601   Figure 8 illustrates more details about the difference in annual emissions between CARS
602   and CAPSS by pollutants and vehicle types. Sedan vehicles show the largest increase of VOC
603   (33%), CO (41%), and NH_3 (23%) in the CARS relative to CAPSS because almost 56% of total
604   vehicle count (13.5 million) is composed of sedan vehicles (Appendix B). In Table 3, sedan
605   vehicles contribute 51% of total VOC and 61% of total CO annual emissions. The VOC and CO
606   emissions from sedans are largely affected by the average speed distribution process when
607   compared to other vehicle types. Similarly, the largest decreases of NO_x (-16%) and SO_x (-18%)
608   are from trucks because they are significant NO_x (~50%) and SO_x contributors (~27%) and their
609   emission factors are sensitive to vehicle speed.

610   **Onroad Emissions Analysis**

611   The CARS is a bottom-up emissions model, which utilizes local individual vehicle activity
612   data, detailed local emission factors for every vehicle and fuel type, and localized inputs such as
613   average speed distribution by road type and deterioration factor. It allows users to assess a detailed
614   breakdown of localized emission contributions. Table 3 represents the individual air pollutants
615   (NO_x, VOC, $PM_{2.5}$, CO, NH_3, and SO_x) emission contributions (t yr^{-1}), fractions (%), and impact
616   factors (IF) by the vehicle type and fuel system. The IF is defined by the normalized annual
617   emissions with vehicle counts of each category (kg yr^{-1} per vehicle). The CARS also can provide

618 the average daily VKT per vehicle, which is the total daily VKT divided by vehicle numbers, to
619 explain the emission contributions in Appendix D.

620 Diesel-fueled vehicles contribute the most NO_x emissions at over 85.3% (257,305 t yr^{-1}),
621 although the number of diesel vehicles only amounts to approximately 35% of the total vehicles
622 (Table 3a). While diesel trucks emitted 49.1% (148,246 t yr^{-1}) of total NO_x with an IF value of
623 47.9 (kg yr^{-1}), the highest impact (IF = 340 kg yr^{-1}) occurred from diesel buses with only an 8.51%
624 contribution to the total NOx emissions. This is caused by the highest average daily VKT from
625 diesel buses compared to other vehicles, which is expected in a highly populated metropolitan area
626 like Seoul, South Korea. A diesel bus generally has a 3-5 times higher daily VKT (180 km d^{-1})
627 than other common vehicles (gasoline sedan: 34 km d^{-1}, diesel truck: 57 km d^{-1}). The second-
628 largest vehicle type is the CNG (compressed natural gas) bus (248 kg yr^{-1}), which also has a high
629 VKT at an average daily of 212 km d^{-1} with only a 3.1% NO_x contribution.

630 For VOC emissions, over 12 million gasoline vehicles cause 52.1% (31,885 t yr^{-1}) of the
631 total VOC emissions, with the gasoline sedan as the highest contributor (46.5% at 14,070 t yr-1)
632 across all vehicle types (Table 3b). Diesel vehicles only contribute 23.0% (14,070 t yr^{-1}) of the
633 total VOC emissions. The IF values from VOC indicate that CNG buses have the highest, which
634 is 247 kg yr^{-1} (19% over total VOC) with a low number of heavy CNG vehicles. The IF of the
635 CNG bus is the highest which is 320 kg yr^{-1} and emits 19.5% of the total VOC. Comparing the IFs
636 of buses across fuel types, the CNG bus emits less NO_x but higher VOC than a diesel vehicle. Each
637 CNG bus has about 33 times higher IF of VOC (320 kg yr^{-1}) than a diesel bus (9.51 kg yr^{-1}), and
638 CNG buses release slightly lower NO_x (248 kg yr^{-1}) than diesel buses (340 kg yr^{-1}) (Table 3a and
639 3b).

640 The South Korea NIER currently does not have the PM emission factors from tire and
641 brake wear, which are the highest contributors of $PM_{2.5}$ emissions from onroad vehicles (Hugo
642 A.C. et al., 2013; Fulvio Amato et al., 2014). Once the emission factors of tire and brake wear are
643 prepared, those emissions can be computed by CARS. For that reason, diesel vehicles become the
644 major source of $PM_{2.5}$ emissions, which contributes over 98.5% (9,959 t yr^{-1}) of the $PM_{2.5}$
645 emissions based on the CARS 2015 emissions (Table 3c). The diesel truck, SUV, and van are three
646 major sources of total $PM_{2.5}$ at 53.6%, 21.4%, and 11.2%, respectively. Although over 52% of the
647 vehicles are gasoline vehicles, their primary $PM_{2.5}$ contribution is limited to 1.44%. The diesel
648 bus has the highest IF (2.83 kg yr^{-1}), which is caused by the largest average daily VKTs.

649 Similar to VOC emissions, CO is mostly emitted through the tailpipe due to incomplete
650 internal combustion of fuel and share similar emissions distributions across vehicle and fuel types
651 (Table 3d). Gasoline vehicles contribute most of the CO (220,390 t yr^{-1}, 59.0%), and sedan vehicles
652 are the primary source (178,121 t yr^{-1}, 47.6%) of this out of all gasoline vehicles. Across vehicle
653 types, buses show the highest IF of CO (81.2 kg yr^{-1}) due to its largest daily VKT. CO is the most
654 abundant pollutant released from vehicles (373,864 t yr^{-1}) across all pollutants from onroad

655 automobile sources. Although CO is much less reactive than other vehicle VOCs (Rinke and
656 Zetzsch, 1984; Liu and Sander, 2015), CO emissions play a critical role in generating 30% of all
657 hydroperoxyl radicals (HO_2) and cause ozone formation in urban areas (Pfister et al., 2019). Thus,
658 CO is also another crucial precursor to ozone formation in urban areas.

659   SO_x emissions are related to the sulfur content within the fuel component. Diesel has the
660 highest sulfur content than any other fuels and consequently most SO_x is contributed by diesel
661 vehicles (93.8 t yr^{-1}, 54.5%) (Table 3e). Within diesel vehicles, trucks provide 26.5% of SO_x (45.
662 t yr^{-1}). Although the SO_x from sedan vehicles are slightly higher (~3.3%) than diesel trucks, the
663 number of diesel trucks is only 29.6% of the number of gasoline sedans. Thus, diesel trucks have
664 a higher IF than gasoline sedans. Across vehicle types, buses have the highest IF (0.095 kg yr^{-1})
665 of SO_x, and diesel buses in particular have the largest IF at 0.143 kg yr^{-1}.

666   The NH_3 emissions table (table 3f) indicates that 98.7% of NH_3 is from gasoline vehicles
667 while diesel trucks only contribute 1.13%. The IF result also shows that the gasoline sedan has the
668 most significant impact per vehicle (1.17 kg yr^{-1}).

669   According to the vehicle activity and the CARS model results, nearly half of the total
670 vehicles (24.3 million) are gasoline sedans (10.4 million, 42.8%), and gasoline sedan vehicles
671 contribute the majority of VOC and CO emissions (46.5% and 47.6%), but only 7.7% of the total
672 NO_x emissions. The number of diesel vehicles is at 8.6 million (35.4%); however, they emit about
673 85.3% of the total NO_x and 98.5% of the primary $PM_{2.5}$. These results indicate that the annual
674 traffic-related automobile emissions are not only affected by the number of vehicles, but also by
675 vehicle and fuel types and age of vehicles. Therefore, this study normalized the annual emissions
676 by the number of vehicles to confirm the emission composition by individual vehicle types.

677 **Average Speed Impact Study**

678   The CARS can also optionally apply the average speed distribution (ASD) by road type to
679 compute more realistic mobile emissions on the road network when compared to using a current
680 single average speed value for each road type (Appendix E). Applying the ASD will generate a
681 better representation of actual traffic patterns from each road type. To understand the impacts of
682 ASD application, we performed sensitivity runs between using a single speed to the ASD
683 application (Appendix F). The ASD data was described in Fig. 4, and the road-specific average
684 single speed values were developed based on the weighted average method using the same ASD
685 data. Appendix E and S6 describe the details of ASD as well as road-specific speed values.

686   Figure 9a shows the differences in total emissions between two scenarios and is organized
687 by pollutant. The single-speed scenario largely underestimates the emissions across all pollutants
688 compared to the ones from the ASD scenario. NO_x (16%), VOC (40%), and CO (30%) were
689 especially underestimated. The difference is caused by the lack of low-speed bins (<16 km h^{-1})
690 representation when a single average speed approach was used. Higher emissions are emitted while

691 vehicles are operated with low-speed bins, which decreases the combustion efficiency of ICE and
692 releases more pollutants.

693   Figure 9b shows the road-specific emissions breakdown between the ASD and single speed
694 approaches to understand the impacts of vehicle operating speeds on onroad automobile emissions.
695 In this figure, each color indicates the emissions percentage differences by road types. Other than
696 NH_3, the most significant discrepancies are from urban local roads, highways, and urban highways,
697 respectively. This pattern is caused by a better presentation of low-speed conditions (<16 km h^{-1})
698 in CAR simulation (Appendix C). The lower speeds cause the incomplete combustion of ICE and
699 increase the emission rate. Also, local urban roads, highways, and urban highways have higher
700 road VKT contributions at 17%, 18%, and 12%, respectively (Appendix C) than rural ones. A
701 better presentation of low-speed operating vehicles from highly travelled roads (urban local, urban
702 highway, and highway) caused these significant differences between the ASD and single-speed
703 approaches. Although the interstate expressway has the largest VKT contribution (41%), it also
704 has the lowest fraction of low-speed bins (2%). That is why the difference between the ASD and
705 single speed scenarios on interstate expressways is less than 1%. In general, NH_3 emission factors
706 do not change by vehicle operating speed, so the ASD impact is quite minimal.

5   Conclusions

708   The CARS is a bottom-up automobile emissions model that utilizes the localized traffic-
709 related activity and emission factors input datasets to generate high quality localized emissions
710 inventories for policymakers, stakeholders, and research community as well as temporally and
711 spatially enhanced hourly gridded emissions for CTMs. First, the CARS model employs the daily
712 VKTs for all registered vehicles and the emission factors function to compute district-level total
713 daily emissions for each vehicle. To reflect realistic traffic patterns, the CARS model computes
714 and utilizes link-level VKTs (=link-length$\times$AADT) from the road network GIS shapefiles to
715 redistribute the original district-level total emissions into spatially enhanced road link-level
716 emissions. It can also optionally implement a control strategy as well as road restriction rules to
717 improve the quality of local emission inventories and meet the needs of users.

718   The CARS model is a fully modularized and computationally optimized python-based
719 model that can effectively process a huge dataset to calculate high quality spatiotemporal county-
720 level, road link-level, and grid cell-level mobile emissions. We believe that the implementation of
721 the ASD into the CARS improves the representation of onroad automobile emissions from the
722 road network when compared to a single speed for each road type. It additionally allows the CARS
723 to have a better representation of low speed (<16 km h-1) vehicle emissions. We believe that CARS
724 model's versatile spatiotemporal bottom-up automobile emissions and the in-depth analysis feature
725 can assist government policymakers and stakeholders to quickly develop responsive emission

726 strategies to South Korea's national PM$_{2.5}$ emergency control strategy that enforces the nationwide
727 vehicle restriction policy within 24 hours.

Code Availability:

729 The source code of the CARS model public release version 1.0 can be downloaded from the
730 Github release website:
731 https://doi.org/10.5281/zenodo.5033314
732
733

Digital Object Identifier (DOI) for the CARS version 1.0:

735 https://doi.org/10.5281/zenodo.5033314
736
737

Installation Package for CARS version 1.0:

739 The CARS version 1.0 installation package comes with the complete inputs and outputs datasets
740 for users to confirm their proper installation on their computers and can be downloaded from the
741 CARS version 1 used in this paper (Baek et al., 2021):
742 https://doi.org/10.5281/zenodo.5033314
743
744

User's Guide Documentation:

746 The CARS version user's guide documentation can be accessed through the the CARS version 1
747 used in this paper (Baek et al., 2021):
748 https://doi.org/10.5281/zenodo.5033314
749

Data availability:

751 All the datasets, excel, and python scripts used in this manuscript for the data analysis are
752 uploaded through GMD website along with a supplemental appendix document.
753

Author contribution

755 Dr. B.H. Baek and Dr. Jung-Hun Woo are the lead researchers in this study. Dr. Rizzieri
756 Pedruzzi developed the source code of CARS model, Dr. Minwoo Park tested the model and
757 provided the model input data. Dr. Chi-Tsan Wang analyzed the model results and prepared the
758 manuscript. Younha Kim and Chul-Han Song also analyzed the model results and provided
759 comments.
760

761

Competing interests

763   The authors declare that they have no conflict of interest.

Acknowledgments

765   This research was funded by the National Strategic Project-Fine Particle of the National Research
766   Foundation (NRF) of Korea funded by the Ministry of Science and ICT (MSIT), the Ministry of
767   Environment (ME), the Ministry of Health and Welfare (MOHW) (NRF-2017M3D8A1092022),
768   and by the Korea Environmental Industry & Technology Institute (KEITI) through the Public
769   Technology Program based on Environmental Policy Program, funded by Korea Ministry of
770   Environment (MOE) (2019000160007).

771

References

Safety flare for burning combustible gas - has tangential inlet for non-flammable gas between housing and stack, in, Shell Oil Co (Shel-C).

Anaconda, Anaconda python: https://www.anaconda.com/products/individual, last access: May, 1st, 2020.

Appel, W., Chemel, C., Roselle, S., Francis, X., Hu, R.-M., Sokhi, R., Rao, S. T., and Galmarini, S.: Examination of the Community Multiscale Air Quality (CMAQ) model performance over the North American and European domains, Atmospheric Environment, 53, 142–155, 10.1016/j.atmosenv.2011.11.016, 2013.

Baek, B. H., Pedruzzi, Rizzieri, Wang, Chi-Tsan, Woo, Jung-Hun (2021). bokhaeng/CARS: CARS (Comprehensive Automobile Emissions Research Simulator) version 1.0 Public Release (CARSv1.0). Zenodo. https://doi.org/10.5281/zenodo.5033314

Baek, B. H., and Seppanen, C., SMOKE v4.8.1 Public Release (January 29, 2021). (Version SMOKEv481_Jan2021): http://doi.org/10.5281/zenodo.4480334.

Burnett, R., Chen, H., Szyszkowicz, M., Fann, N., Hubbell, B., Pope, C. A., Apte, J. S., Brauer, M., Cohen, A., Weichenthal, S., Coggins, J., Di, Q., Brunekreef, B., Frostad, J., Lim, S. S., Kan, H., Walker, K. D., Thurston, G. D., Hayes, R. B., Lim, C. C., Turner, M. C., Jerrett, M., Krewski, D., Gapstur, S. M., Diver, W. R., Ostro, B., Goldberg, D., Crouse, D. L., Martin, R. V., Peters, P., Pinault, L., Tjepkema, M., van Donkelaar, A., Villeneuve, P. J., Miller, A. B., Yin, P., Zhou, M., Wang, L., Janssen, N. A. H., Marra, M., Atkinson, R. W., Tsang, H., Quoc Thach, T., Cannon, J. B., Allen, R. T., Hart, J. E., Laden, F., Cesaroni, G., Forastiere, F., Weinmayr, G., Jaensch, A., Nagel, G., Concin, H., and Spadaro, J. V.: Global estimates of mortality associated with long-term exposure to outdoor fine particulate matter, Proceedings of the National Academy of Sciences, 115, 9592, 10.1073/pnas.1803222115, 2018.

Choi, D., Beardsley, M., Brzezinski, D., Koupal, J., and Warila, J.: MOVES Sensitivity Analysis: The Impacts of Temperature and Humidity on Emissions
, available at: https://www3.epa.gov/ttn/chief/conference/ei19/session6/choi.pdf 2017.

Choi, K.-C., Lee, J.-J., Bae, C. H., Kim, C.-H., Kim, S., Chang, L.-S., Ban, S.-J., Lee, S.-J., Kim, J., and Woo, J.-H.: Assessment of transboundary ozone contribution toward South Korea using

802 multiple source–receptor modeling techniques, Atmospheric Environment, 92, 118-129,
803 https://doi.org/10.1016/j.atmosenv.2014.03.055, 2014.

804 Cohen, A. J., Brauer, M., Burnett, R., Anderson, H. R., Frostad, J., Estep, K., Balakrishnan, K.,
805 Brunekreef, B., Dandona, L., Dandona, R., Feigin, V., Freedman, G., Hubbell, B., Jobling, A.,
806 Kan, H., Knibbs, L., Liu, Y., Martin, R., Morawska, L., Pope, C. A., III, Shin, H., Straif, K.,
807 Shaddick, G., Thomas, M., van Dingenen, R., van Donkelaar, A., Vos, T., Murray, C. J. L., and
808 Forouzanfar, M. H.: Estimates and 25-year trends of the global burden of disease attributable to
809 ambient air pollution: an analysis of data from the Global Burden of Diseases Study 2015, The
810 Lancet, 389, 1907-1918, 10.1016/S0140-6736(17)30505-6, 2017.
811

812 Dennis, R., Fox, T., Fuentes, M., Gilliland, A., Hanna, S., Hogrefe, C., Irwin, J., Rao, S. T.,
813 Scheffe, R., Schere, K., Steyn, D., and Venkatram, A.: A FRAMEWORK FOR EVALUATING
814 REGIONAL-SCALE NUMERICAL PHOTOCHEMICAL MODELING SYSTEMS, Environ
815 Fluid Mech (Dordr), 10, 471-489, 10.1007/s10652-009-9163-2, 2010.

816 EEA: EMEP/EEO air pollutant emission inventory guidebook 2016, 2019.

817 Enthought, Enthought Canapy Python: https://assets.enthought.com/downloads/edm/, last
818 access: May, 1st, 2020.

819 Fallahshorshani, M., André, M., Bonhomme, C., and Seigneur, C.: Coupling Traffic, Pollutant
820 Emission, Air and Water Quality Models: Technical Review and Perspectives, Procedia - Social
821 and Behavioral Sciences, 48, 1794-1804, https://doi.org/10.1016/j.sbspro.2012.06.1154, 2012.

822 Fulvio Amato, Flemming R. Cassee, Hugo A.C. Denier van der Gon, Robert Gehrig, Mats
823 Gustafsson, Wolfgang Hafner, Roy M. Harrison, Magdalena Jozwicka, Frank J. Kelly,
824 TeresaMoreno, Andre S.H. Prevot, Martijn Schaap, Jordi Sunyer, Xavier Querol, Urban air
825 quality:The challenge of traffic non-exhaust emissions, Journal of Hazardous Materials, 275, 31-
826 36, https://doi.org/10.1016/j.jhazmat.2014.04.053, 2014.
827

828 Guevara, M., Tena, C., Porquet, M., Jorba, O., and Pérez García-Pando, C.: HERMESv3, a
829 stand-alone multi-scale atmospheric emission modelling framework – Part 1: global and regional
830 module, Geosci. Model Dev., 12, 1885-1907, 10.5194/gmd-12-1885-2019, 2019.

831 Hogrefe, C., Rao, S. T., Kasibhatla, P., Hao, W., Sistla, G., Mathur, R., and McHenry, J.:
832 Evaluating the performance of regional-scale photochemical modeling systems: Part II—ozone

833   predictions, Atmospheric Environment, 35, 4175-4188, https://doi.org/10.1016/S1352-
834   2310(01)00183-2, 2001a.

835   Hogrefe, C., Rao, S. T., Kasibhatla, P., Kallos, G., Tremback, C. J., Hao, W., Olerud, D., Xiu,
836   A., McHenry, J., and Alapaty, K.: Evaluating the performance of regional-scale photochemical
837   modeling systems: Part I—meteorological predictions, Atmospheric Environment, 35, 4159-
838   4174, https://doi.org/10.1016/S1352-2310(01)00182-0, 2001b.

839   Hugo A.C. Denier van der Gon, Miriam E. Gerlofs-Nijland, Robert Gehrig, Mats Gustafsson,
840   Nicole Janssen, Roy M. Harrison, Jan Hulskotte, Christer Johansson, Magdalena Jozwicka,
841   Menno Keuken, Klaas Krijgsheld, Leonidas Ntziachristos, Michael Riediker & Flemming R.
842   Cassee: The Policy Relevance of Wear Emissions from Road Transport, Now and in the
843   Future—An International Workshop Report and Consensus Statement, Journal of the Air &
844   Waste Management Association, 63:2, 136-149, DOI: 10.1080/10962247.2012.741055, 2013
845

846   Ibarra-Espinosa, S., Ynoue, R., amp, apos, Sullivan, S., Pebesma, E., Andrade, M. d. F., and
847   Osses, M.: VEIN v0.2.2: an R package for bottom–up vehicular emissions inventories, Geosci.
848   Model Dev., 11, 2209-2229, 10.5194/gmd-11-2209-2018, 2018a.

849   Ibarra-Espinosa, S., Ynoue, R., O'Sullivan, S., Pebesma, E., Andrade, M. D. F., and Osses, M.:
850   VEIN v0.2.2: an R package for bottom–up vehicular emissions inventories, Geosci. Model Dev.,
851   11, 2209-2229, 10.5194/gmd-11-2209-2018, 2018b.

852   IEMA, Inventário de Emissões Atmosféricas do Transporte Rodoviário de Passageiros no
853   Município de São Paulo.: http://emissoes.energiaeambiente.org.br, last access: May,1st, 2017.

854   Jang, Y. K., Cho, K. L., Kim, K., Kim, H. J., and Kim, J.: Development of methodology for
855   esimation of air pollutants emissions and future emissions from on-road mobile sources.,
856   National Institute of Environmental Research, Incheon, Korea., available at: 2007.

857   Kaewunruen, S., Sussman, J. M., and Matsumoto, A.: Grand Challenges in Transportation and
858   Transit Systems, Frontiers in Built Environment, 2, 10.3389/fbuil.2016.00004, 2016.

859   Kim, B.-U., Bae, C., Kim, H. C., Kim, E., and Kim, S.: Spatially and chemically resolved source
860   apportionment analysis: Case study of high particulate matter event, Atmospheric Environment,
861   162, 55-70, https://doi.org/10.1016/j.atmosenv.2017.05.006, 2017a.

862 Kim, H. C., Kim, E., Bae, C., Cho, J. H., Kim, B. U., and Kim, S.: Regional contributions to
863 particulate matter concentration in the Seoul metropolitan area, South Korea: seasonal variation
864 and sensitivity to meteorology and emissions inventory, Atmos. Chem. Phys., 17, 10315-10332,
865 10.5194/acp-17-10315-2017, 2017b.

866 Kim, H. C., Kim, S., Kim, B.-U., Jin, C.-S., Hong, S., Park, R., Son, S.-W., Bae, C., Bae, M.,
867 Song, C.-K., and Stein, A.: Recent increase of surface particulate matter concentrations in the
868 Seoul Metropolitan Area, Korea, Scientific Reports, 7, 4710, 10.1038/s41598-017-05092-8,
869 2017c.

870 L., W. P., and Heo, G.: Development of revised SAPRC aromatics mechanism, available at:
871 https://www.engr.ucr.edu/~carter/SAPRC/saprc11.pdf 2012.

872 Lee, D., Lee, Y.-M., Jang, K.-W., Yoo, C., Kang, K.-H., Lee, J.-H., Jung, S.-W., Park, J.-M.,
873 Lee, S.-B., Han, J.-S., Hong, J.-H., and Lee, S.-J.: Korean National Emissions Inventory System
874 and 2007 Air Pollutant Emissions, Asian Journal of Atmospheric Environment, 5-4, 278-291,
875 2011a.

876 Lee, D.-G., Lee, Y.-M., Jang, K.-W., Yoo, C., Kang, K.-H., Lee, J.-H., Jung, S.-W., Park, J.-M.,
877 Lee, S.-B., Han, J.-S., Hong, J.-H., and Lee, S.-J.: Korean National Emissions Inventory System
878 and 2007 Air Pollutant Emissions, Asian Journal of Atmospheric Environment, 5,
879 10.5572/ajae.2011.5.4.278, 2011b.

880 Lejri, D., Can, A., Schiper, N., and Leclercq, L.: Accounting for traffic speed dynamics when
881 calculating COPERT and PHEM pollutant emissions at the urban scale, Transportation Research
882 Part D: Transport and Environment, 63, 588-603, https://doi.org/10.1016/j.trd.2018.06.023,
883 2018.

884 Li, F., Zhuang, J., Cheng, X., Li, M., Wang, J., and Yan, Z.: Investigation and Prediction of
885 Heavy-Duty Diesel Passenger Bus Emissions in Hainan Using a COPERT Model, Atmosphere,
886 10, 106, 10.3390/atmos10030106, 2019.

887 Li, Q., Qiao, F., and yu, L.: Vehicle Emission Implications of Drivers Smart Advisory System
888 for Traffic Operations in Work Zones, Journal of the Air & Waste Management Association, 11,
889 10.1080/10962247.2016.1140095, 2016.

890 Liu, H., Guensler, R., Lu, H., Xu, Y., Xu, X., and Rodgers, M.: MOVES-Matrix for High-
891 Performance On-Road Energy and Running Emission Rate Modeling Applications, Journal of
892 the Air & Waste Management Association, 69, 10.1080/10962247.2019.1640806, 2019.

893 Liu, Y., and Sander, S. P.: Rate Constant for the OH + CO Reaction at Low Temperatures, The
894 Journal of Physical Chemistry A, 119, 10060-10066, 10.1021/acs.jpca.5b07220, 2015.

895 Luo, H., Astitha, M., Hogrefe, C., Mathur, R., and Rao, S. T.: A new method for assessing the
896 efficacy of emission control strategies, Atmospheric Environment, 199, 233-243,
897 https://doi.org/10.1016/j.atmosenv.2018.11.010, 2019.

898 Lv, W., Hu, Y., Li, E., Liu, H., Pan, H., Ji, S., Hayat, T., Alsaedi, A., and Ahmad, B.: Evaluation
899 of vehicle emission in Yunnan province from 2003 to 2015, J. Clean Prod., 207, 814-825,
900 https://doi.org/10.1016/j.jclepro.2018.09.227, 2019.

901 Moussiopoulos, N., Vlachokostas, C., Tsilingiridis, G., Douros, I., Hourdakis, E., Naneris, C.,
902 and Sidiropoulos, C.: Air quality status in Greater Thessaloniki Area and the emission reductions
903 needed for attaining the EU air quality legislation, Sci. Total Environ., 407, 1268-1285,
904 https://doi.org/10.1016/j.scitotenv.2008.10.034, 2009.

905 Nagpure, A. S., Gurjar, B. R., Kumar, V., and Kumar, P.: Estimation of exhaust and non-exhaust
906 gaseous, particulate matter and air toxics emissions from on-road vehicles in Delhi, Atmospheric
907 Environment, 127, 118-124, 10.1016/j.atmosenv.2015.12.026, 2016.

908 NIER: Study on Air Pollutant Emission Estimation Method in Transportation section(II) 11-
909 1480523-003573-01, National Archives of Korea, available at:
910 https://www.archives.go.kr/next/manager/publishmentSubscriptionDetail.do?prt_seq=114054&p
911 age=1554&prt_arc_title=&prt_pub_kikwan=&prt_no 2018.

912 Ntziachristos, L., and Samaras, Z.: Speed-dependent representative emission factors for catalyst
913 passenger cars and influencing parameters, Atmospheric Environment, 34, 4611-4619,
914 https://doi.org/10.1016/S1352-2310(00)00180-1, 2000.

915 Ntziachristos, L., Gkatzoflias, D., Kouridis, C., and Samaras, Z.: COPERT: A European road
916 transport emission inventory model, 491-504 pp., 2009.

917 Pedruzzi, R., Baek, B. H., and Wang, C.-T., CARS: https://github.com/CMASCenter/CARS,
918 last access: MAy, 1st, 2020.

919 Perugu, H., Ramirez, L., and DaMassa, J.: Incorporating temperature effects in California's on-
920 road emission gridding process for air quality model inputs, Environ Pollut, 239, 1-12,
921 10.1016/j.envpol.2018.03.094, 2018.

922   Perugu, H.: Emission modelling of light-duty vehicles in India using the revamped VSP-based
923   MOVES model: The case study of Hyderabad, Transportation Research Part D: Transport and
924   Environment, 68, 150-163, https://doi.org/10.1016/j.trd.2018.01.031, 2019.

925   Pfister, G., Wang, C.-t., Barth, M., Flocke, F., Vizuete, W., and Walters, S.: Chemical
926   Characteristics and Ozone Production in the Northern Colorado Front Range, JGR, 2019.

927   Pinto, J. A., Kumar, P., Alonso, M. F., Andreão, W. L., Pedruzzi, R., dos Santos, F. S., Moreira,
928   D. M., and Albuquerque, T. T. d. A.: Traffic data in air quality modeling: A review of key
929   variables, improvements in results, open problems and challenges in current research,
930   Atmospheric Pollution Research, 11, 454-468, https://doi.org/10.1016/j.apr.2019.11.018, 2020.

931   Rao, S. T., Galmarini, S., and Puckett, K.: Air Quality Model Evaluation International Initiative
932   (AQMEII): Advancing the State of the Science in Regional Photochemical Modeling and Its
933   Applications, Bulletin of the American Meteorological Society, 92, 23-30,
934   10.1175/2010BAMS3069.1, 2011.

935   Rodriguez-Rey et al. (2021): Rodriguez-Rey, D., Guevara, M., Linares, MP., Casanovas, J.,
936   Salmerón, J., Soret, A.,Jorba, O., Tena, C., Pérez García-Pando, C.: A coupled macroscopic
937   traffic and pollutant emission modelling system for Barcelona, Transportation Research Part D,
938   92, https://doi.org/10.1016/j.trd.2021.102725, 2021.

939   Rinke, M., and Zetzsch, C.: Rate Constants for the Reactions of OH Radicals with Aromatics:
940   Benzene, Phenol, Aniline, and 1,2,4-Trichlorobenzene, Berichte der Bunsengesellschaft für
941   physikalische Chemie, 88, 55-62, 10.1002/bbpc.19840880114, 1984.

942   Russell, A., and Dennis, R.: NARSTO critical review of photochemical models and modeling,
943   Atmospheric Environment, 34, 2283-2324, https://doi.org/10.1016/S1352-2310(99)00468-9,
944   2000.

945   Ryu, J. H., Han, J. S., Lim, C. S., Eom, M. D., Hwang, J. W., Yu, S. H., Lee, T. W., Yu, Y. S.,
946   and Kim, G. H.: The Study on the Estimation of Air Pollutants from Auto- mobiles (I) -
947   Emission Factor of Air Pollutants from Middle and Full sized Buses., in, Transportation
948   Pollution Research Center, National Institute of Environmental Research, Incheon, Korea., 2003.

949   Ryu, J. H., Lim, C. S., Yu, Y. S., Han, J. S., Kim, S. M., Hwang, J. W., Eom, M. D., Kim, G. Y.,
950   Jeon, M. S., Kim, Y. H., Lee, J. T., and Lim, Y. S.: The Study on the Esti- mation of Air
951   Pollutants from Automobiles (II) - Emis- sion Factor of Air Pollutants from Diesel Truck., in,

952   Trans- portation Pollution Research Center, National Institute of Environmental Research,
953   Incheon, Korea., 2004.

954   Ryu, J. H., Yu, Y. S., Lim, C. S., Kim, S. M., Kim, J. C., Gwon, S. I., Jeong, S. W., and Kim, D.
955   W.: The Study on the Estimation of Air Pollutants from Automobiles (III) - Emission Factor of
956   Air Pollutants from Small sized Light-duty Vehicles., in, Transportation Pollution Research
957   Center, National Institute of Environmental Research, Korea., 2005.

958   Sallis, P., Bull, F., Burdett, P., Frank, P., Griffiths, P., Giles-Corti, P., and Stevenson, M.: Use of
959   science to guide city planning policy and practice: How to achieve healthy and sustainable future
960   cities, The Lancet, 388, 10.1016/S0140-6736(16)30068-X, 2016.

961   Smit, R., Kingston, P., Neale, D. W., Brown, M. K., Verran, B., and Nolan, T.: Monitoring on-
962   road air quality and measuring vehicle emissions with remote sensing in an urban area,
963   Atmospheric Environment, 218, 116978, https://doi.org/10.1016/j.atmosenv.2019.116978, 2019.

964   Sun, W., Duan, N., Yao, R., Huang, J., and Hu, F.: Intelligent in-vehicle air quality
965   management : a smart mobility application dealing with air pollution in the traffic, 2016.

966   Tominaga, Y., and Stathopoulos, T.: Ten questions concerning modeling of near-field pollutant
967   dispersion in the built environment, Build. Environ., 105, 390-402,
968   https://doi.org/10.1016/j.buildenv.2016.06.027, 2016.

969   USEPA: Population and Activity of Onroad Vehicles in MOVES3, in, edited by: USEPA, 2020.

970   WHO, Ambient air pollution- a major threat to health and climate:
971   https://www.who.int/airpollution/ambient/en/, last 2019.

972   Xu, X., Liu, H., Anderson, J. M., Xu, Y., Hunter, M. P., Rodgers, M. O., and Guensler, R. L.:
973   Estimating Project-Level Vehicle Emissions with Vissim and MOVES-Matrix, Transportation
974   Research Record, 2570, 107-117, 10.3141/2570-12, 2016.

975   Yarwood, G., and Jung, J.: UPDATES TO THE CARBON BOND MECHANISM FOR
976   VERSION 6 (CB6), 2010.
977

978 **Tables**

979 **Table 1**. Computational processing time by CARS module based on the modeling setup: Total
980 number of activity data = 24,383,578; Emission Factors = 84,608; GIS road links=385,795;
981 districts/states=5,150/16; 9km×9km grid cells=5,494 (82 columns× 67 columns).

No	Module	Desktop i7 (minutes)	Laptop i9 (minutes)	Averaged Time (minutes)
1	**Process activity data**	1.8	1.5	1.7
2	**process emission factors**	1.1	0.8	1.0
3	**Process shape file**	9.9	7.3	8.6
4	**Calculate district emissions**	6.4	5.7	6.1
5	**Grid4AQM** [31days]	4.8 [75.9]	5.0 [87.2]	4.9 [81.6]
6	**Plot figures**	6.2	5.4	5.8
	Total [31days]	30.2 [101.3]	25.7 [107.9]	28.1[104.8]

982
983
984

985 **Table 2**. The total emissions comparison between CARS and CAPSS for the 2015 emission.

Emission Inventory	Pollutants (t yr^{-1})					
	NO$_x$	VOC	PM2.5	CO	SO$_x$	NH$_3$
CARS 2015	**301,794**	**61,186**	**10,108**	**373,864**	**172**	**12,453**
CAPSS 2015	369,585	46,145	8,817	245,516	209	10,079

986

987

988 **Table 3**. The summary tables of emissions (t yr^{-1}), contributions (%), and impact factor (IF, kg yr^{-}

989 ^{1}) per vehicle for criteria air pollutants (CAPs) by vehicle and fuel types: (a) for NO$_x$; (b) VOC;

990 (c) for PM$_{2.5}$; (d) for CO; (e) for SO$_x$; and (f) for NH$_3$.

991

992 (a) NOx

Vehicle	Gasoline		Diesel		LPG		CNG		Hybrid		Total	
	Emission	IF	Emission	IF	Emission	IF	Emission	IF	Emission	IF	Emission	IF
Sedan	20,219 (6.70%)	1.94	14,783 (4.90%)	12.8	8,159 (2.77%)	4.49	12 (0.00%)	1.26	65 (0.02%)	0.39	43,239 (14.3%)	3.19
Truck	23 (0.01%)	5.54	**148,246 (49.1%)**	47.9	920 (0.31%)	4.55	88 (0.03%)	66.4	-	-	**149,277 (49.5%)**	45.2
Bus	0 (0.00%)	0.97	25,677 (8.51%)	**340**	-	-	9,260 (3.07%)	248	0 (0.00%)	1.77	34,938 (11.6%)	**333**
SUV	159 (0.05%)	1.19	39,565 (13.1%)	11.4	175 (0.06%)	8.54	0 (0.00%)	1.60	1 (0.00%)	0.42	39,900 (13.2%)	11.0
Van	14 (0.00%)	4.78	16,659 (5.52%)	22.6	1,337 (0.44%)	6.80	0 (0.00%)	1.25	0 (0.00)	0.37	18,012 (6.00%)	19.2
Taxi	-	-	-	-	1,217 (0.40%)	2.11	-	-	-	-	1,217 (0.40%)	2.11
Special	1 (0.00%)	20.1	12,347 (4.10%)	152	0 (0.00%)	0.52	-	-	-	-	12,375 (4.10%)	151
Motorcycle	2,836 (0.94%)	1.31	-		-	-	-	-	-	-	2,836 (0.94%)	1.32
Total	23,253 (7.70%)	1.83	**257,305 (85.3%)**	29.9	11,809 (3.91%)	4.20	9,361 (3.10%)	**36.7**	66 (0.02%)	0.39	301,794 (100%)	13.3

993

994 (b) VOC

Vehicle	Gasoline		Diesel		LPG		CNG		Hybrid		Total	
	Emission	IF	Emission	IF	Emission	IF	Emission	IF	Emission	IF	Emission	IF
Sedan	28,434 (46.5%)	2.73	629 (1.03%)	0.55	2,107 (3.44%)	1.16	3 (0.01%)	0.33	77 (0.13%)	0.47	**31,250 (51.1%)**	2.30
Truck	23 (0.04%)	5.44	8,194 (13.4%)	2.65	286 (0.47%)	1.41	102 (0.17%)	77.2	-	-	8,605 (14.1%)	2.61
Bus	0 (0.00%)	1.65	717 (1.17%)	9.51	-	-	11,942 (19.5%)	320	0 (0.00%)	0	12,659 (20.7%)	**112**
SUV	246 (0.40%)	1.84	2,441 (3.99%)	0.71	46 (0.08%)	2.25	0 (0.00%)	0.75	1 (0.00%)	0.55	2,733 (4.47%)	0.76
Van	21 (0.03%)	7.04	1,185 (1.94%)	1.61	393 (0.64%)	2.00	0 (0.00%)	0.45	0 (0.00%)	0	1,599 (2.61%)	1.71
Taxi	-	-	-	-	273 (0.45%)	0.47	-	-	-	-	273 (0.45%)	0.47
Special	1 (0.00%)	25.8	904 (1.48%)	11.1	0 (0.00%)	0.23	-	-	-	-	905 (1.48%)	11.0
Motorcycle	3,160 (5.16%)	1.46	-		-	-	-	-	-	-	3,160 (5.16%)	1.46
Total	**31,885 (52.1%)**	2.50	14,070 (23.0%)	1.64	3,106 (5.08%)	1.10	12,047 (19.7%)	**247**	78 (0.13%)	0.47	61,186 (100%)	2.51

995

996 (c) PM2.5

Vehicle	Gasoline		Diesel		LPG		CNG		Hybrid		Total	
	Emission	IF	Emission	IF	Emission	IF	Emission	IF	Emission	IF	Emission	IF
Sedan	144 (1.42%)	0.01	809 (8.00%)	0.70	0	0	0	0	3 (0.03%)	0.02	956 (9.46%)	0.07
Truck	0 (0.01%)	0	**5,415 (53.6%)**	1.75	0	0	0	0	-	-	**5,415 (53.6%)**	1.64
Bus	0	0	214 (2.11%)	**2.83**	-	-	0	0	0 (0.01%)	0.09	214 (2.11%)	1.89
SUV	2 (0.02%)	0.02	2,165 (21.4%)	0.63	0	0	0	0	0	0.02	2,167 (21.4%)	0.60
Van	0	0	1,127 (11.2%)	1.53	0	0	0	0	0	0.02	1,127 (11.2%)	1.20
Taxi	-	-	-	-	0	0	-	-	-	-	0	0
Special	0	0	230 (2.28%)	2.82	0	0	-	-	-	-	230 (2.28%)	**2.81**
Motorcycle	0	0	-		-	-	-	-	-	-	0	0
Total	146 (1.44%)	0.01	**9,959 (98.5%)**	**1.16**	0	0	0	0	3 (0.03%)	0.02	10,108 (100%)	0.41

997
998

(d) CO

Vehicle	Gasoline		Diesel		LPG		CNG		Hybrid		Total	
	Emission	IF	Emission	IF	Emission	IF	Emission	IF	Emission	IF	Emission	IF
Sedan	178,121 (47.6%)	17.1	3,436 (0.92%)	2.98	42,886 (11.5%)	23.6	29 (0.01%)	2.91	177 (0.05%)	1.07	**224,649 (60.1%)**	16.6
Truck	254 (0.07%)	61.1	47,065 (12.6%)	15.2	9,088 (2.43%)	44.9	68 (0.02%)	51.4	-	-	56,475 (15.1%)	17.1
Bus	0 (0.00%)	19.3	7,633 (2.05%)	**101**	-	-	1542 (0.41%)	41.3	1 (0.00%)	4.64	9,176 (2.45%)	**81.2**
SUV	2,616 (0.70%)	19.6	13,401 (3.58%)	3.87	791 (0.21%)	38.6	0 (0.00%)	4.09	2 (0.00%)	1.15	16,808 (4.50%)	4.65
Van	131 (0.04%)	43.4	6,611 (1.77%)	8.97	8,032 (2.15%)	40.9	2 (0.00%)	6.53	0 (0.00%)	1.00	14,777 (3.95%)	15.8
Taxi	-	-	-	-	8,481 (2.27%)	14.7	-	-	-	-	8,481 (2.27%)	14.7
Special	13 (0.00%)	269	4,224 (1.13%)	51.7	1 (0.00%)	3.69	-	-	-	-	4,239 (1.13%)	51.7
Motorcycle	39,256 (10.5%)	18.2	-		-	-	-	-	-	-	39,256 (10.5%)	18.2
Total	**220,390 (59.0%)**	17.3	82,372 (22.0%)	9.57	69,281 (18.5%)	**24.6**	1641 (0.44%)	33.6	180 (0.05%)	1.07	373,864 (100%)	15.4

(e) SO$_x$

Vehicle	Gasoline		Diesel		LPG		CNG		Hybrid		Total	
	Emission	IF	Emission	IF	Emission	IF	Emission	IF	Emission	IF	Emission	IF
Sedan	51.3 (29.8%)	0.005	6.5 (3.79%)	0.006	8.28 (4.81%)	0.005	0	0	1.14 (0.67%)	0.007	**67.2 (39.1%)**	0.005
Truck	0.03 (0.02%)	0.008	45.5 (26.5%)	0.015	0.97 (0.57%)	0.005	0	0	-	-	46.5 (27.1%)	0.014
Bus	0 (0.00%)	0.003	10.8 (6.26%)	**0.143**	-	-	0	0	0.01 (0.01%)	0.047	10.8 (6.26%)	**0.095**
SUV	0 (0.00%)	0.000	18.2 (10.6%)	0.005	0.00 (0.00%)	0.000	0	0	0.01 (0.01%)	0.007	18.2 (10.6%)	0.005
Van	0.02 (0.01%)	0.006	5.5 (3.20%)	0.007	0.77 (0.45%)	0.004	0	0	0 (0.00%)	0.010	6.30 (3.66%)	0.007
Taxi	-	-	-	-	7.71 (4.49%)	0.013	-	-	-	-	7.71 (4.48%)	0.013
Special	0 (0.00%)	0.003	7.3 (4.27%)	0.090	0.00 (0.00%)	0.005	-	-	-	-	7.34 (4.27%)	0.090
Motorcycle	7.94 (4.62%)	0.004	-		-	-	-	-	-	-	7.94 (4.62%)	0.004
Total	59.3 (34.5%)	0.006	**93.8 (54.5%)**	**0.011**	17.7 (10.3%)	0.006	0	0	1.17 (0.68%)	0.007	172 (100%)	0.007

(e) NH$_3$

Vehicle	Gasoline		Diesel		LPG		CNG		Hybrid		Total	
	Emission	IF	Emission	IF	Emission	IF	Emission	IF	Emission	IF	Emission	IF
Sedan	12,225 (98.3%)	**1.17**	20 (0.16%)	0.02	0	0.00	0	0	19 (0.15%)	0.11	**12,284 (98.6%)**	**0.91**
Truck	0 (0.00%)	0.03	82 (0.66%)	0.03	0	0.00	0	0	-	-	82 (0.66%)	0.02
Bus	0 (0.00%)	0.09	15 (0.12%)	0.19	-	-	0	0	0 (0.00%)	0.51	15 (0.12%)	0.13
SUV	0 (0.00%)	0.00	0 (0.00%)	0.00	0	0.00	0	0	0 (0.00%)	0.16	0 (0.00%)	0.00
Van	0 (0.00%)	0.02	14 (0.11%)	0.02	0	0.00	0	0	0 (0.00%)	0.09	14 (0.11%)	0.01
Taxi	-	-	-	-	0	0.00	-	-	-	-	0 (0.00%)	0.00
Special	0 (0.00%)	0.01	10 (0.08%)	0.12	0	0.00	-	-	-	-	10 (0.08%)	0.12
Motorcycle	49 (0.39%)	0.02	-		-	-	-	-	-	-	49 (0.39%)	0.02
Total	**12,293 (98.7%)**	**0.97**	141 (1.13%)	0.02	0	0.00	0	0	19 (0.16%)	0.12	12,453 (100%)	0.51

1008 **Figures**
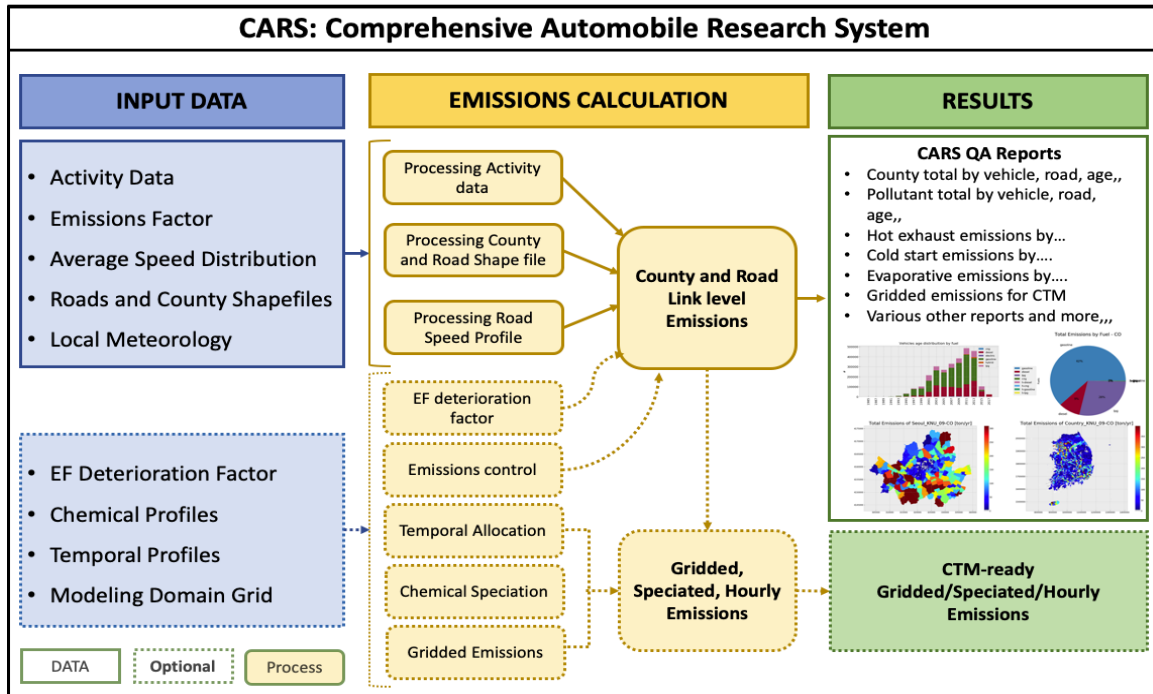
1009

1010 **Figure 1**. CARS schematic methodology to estimate mobile emissions.

1011
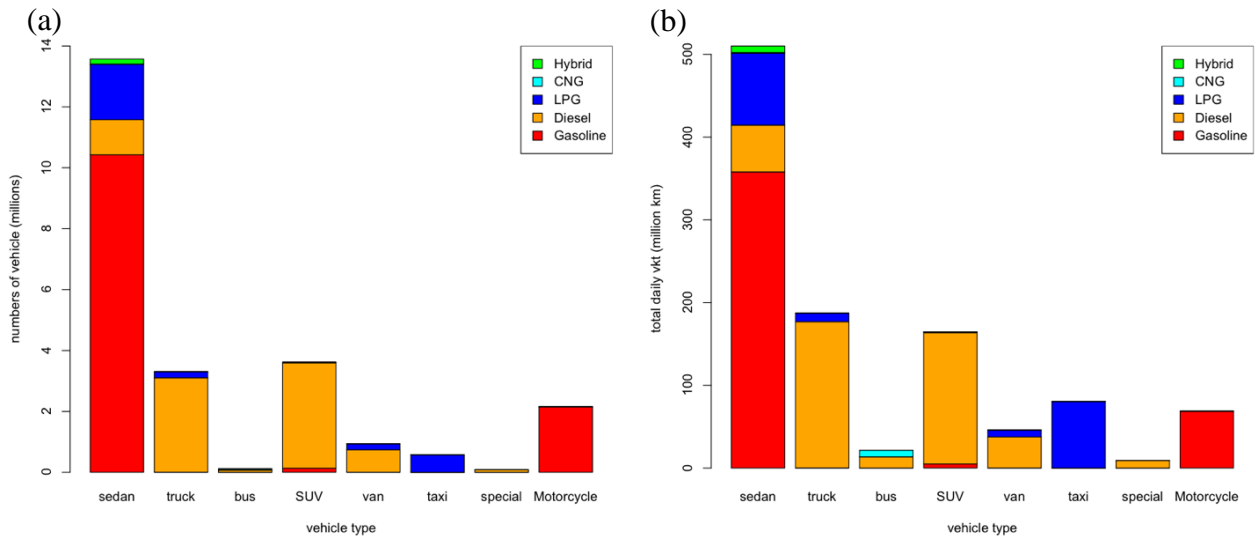
1012

1013   **Figure 2. (a)** The number of vehicles by vehicle and fuel types and **(b)** the total daily VKT by

1014   vehicle and fuel types in South Korea.

1015

1016
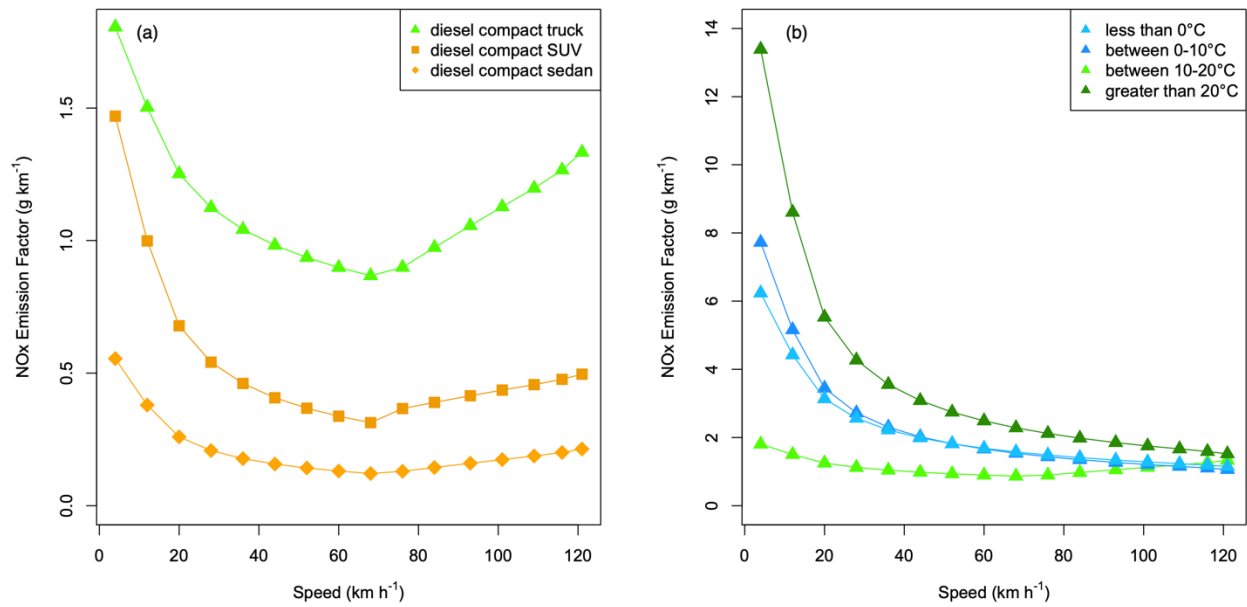
1017

1018 **Figure 3**. Variation of NOx emission factors from diesel compact engines by vehicle speed and
1019 ambient temperatures: **(a)** NO_x emission factors function to vehicle speed; **(b)** NO_x emission
1020 factors of diesel compact truck function to vehicle speed and ambient temperature.

1021
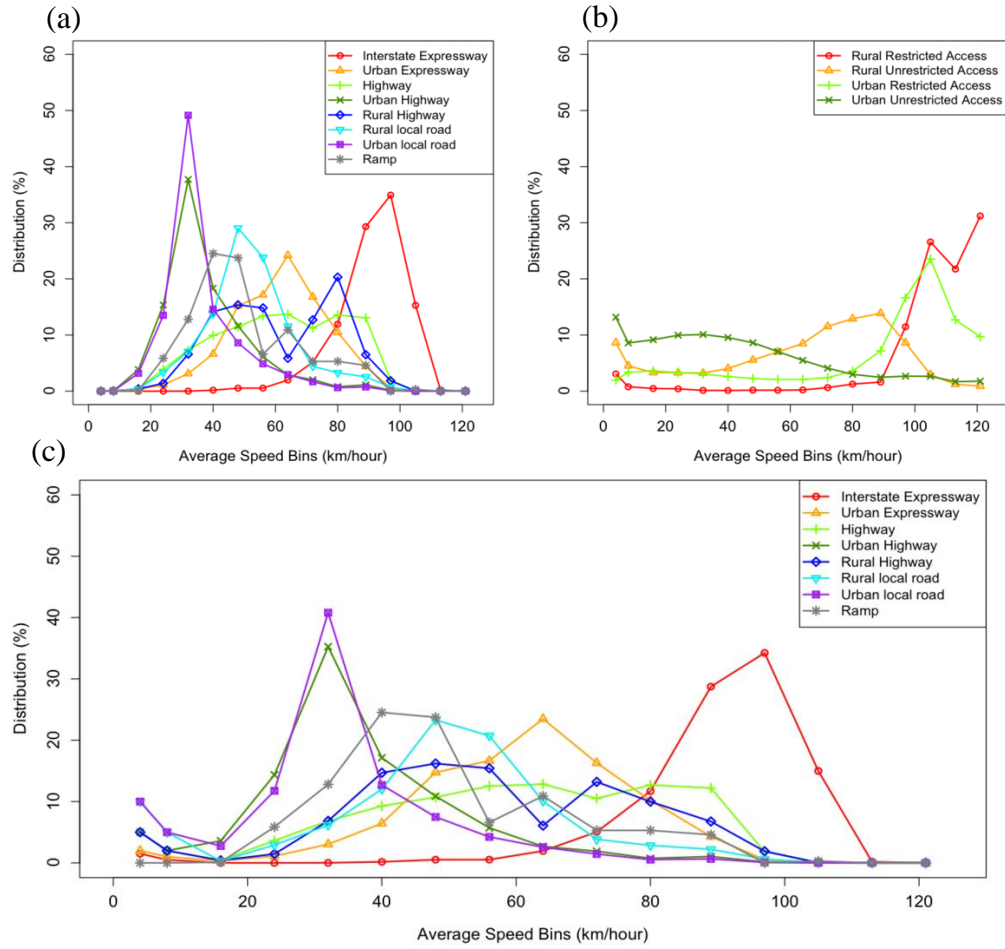
1022

1023

Figure 4. (a) The South Korea speed distribution by road types. (b) The Georgia state speed distribution by road types. (c) The average speed distribution (ASD) by road types used in this study for South Korea.

1024
1025
1026
1027
1028
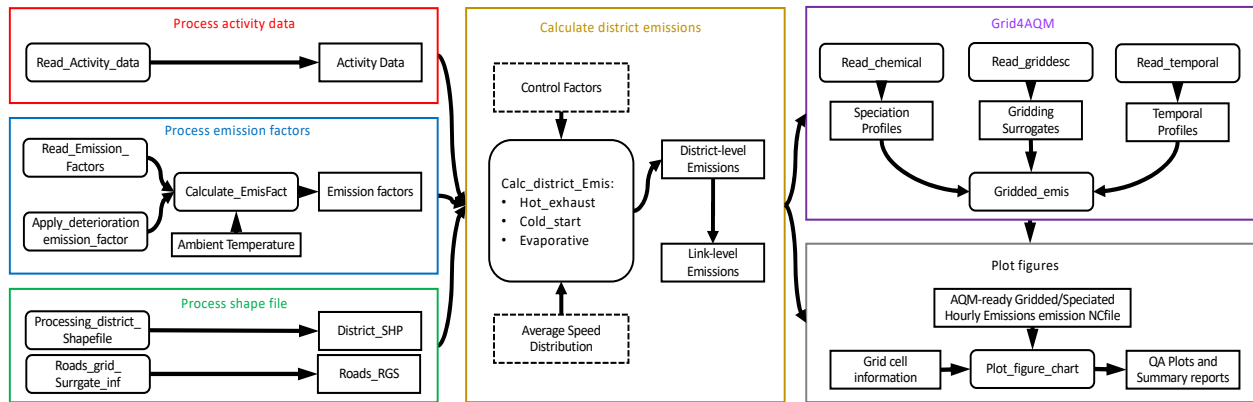
1029
1030 **Figure 5**. The schematic of modules and their functions in the CARS.
1031
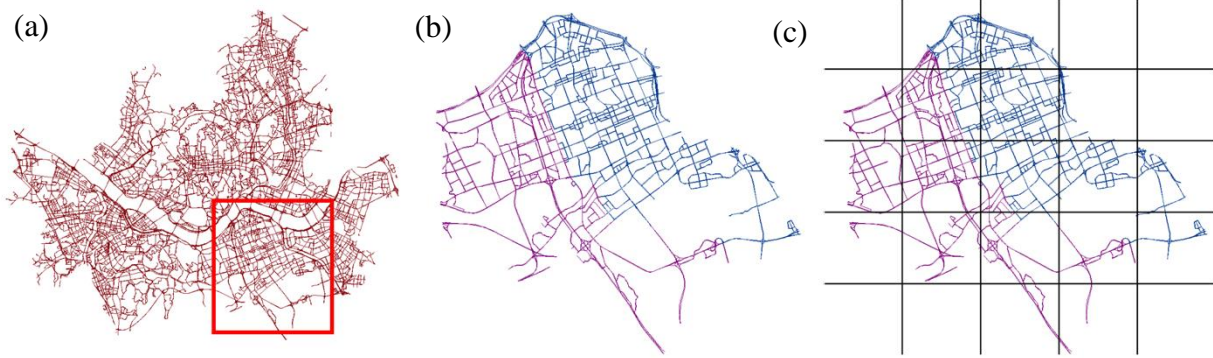
1032

1033 **Figure 6 (a)** the road network GIS shapefile of Seoul, South Korea; **(b)** two districts with different

1034 colors (purple and blue); **(c)** the modeling grid cells over road segments.

1035
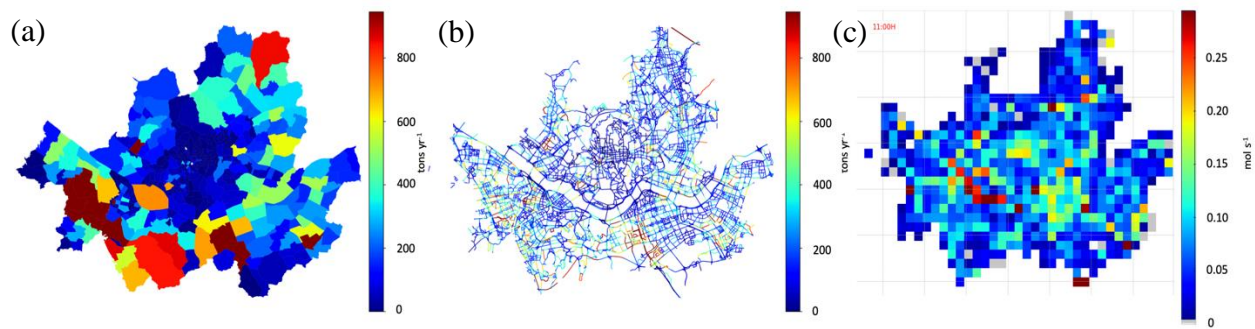
1036

1037   **Figure 7**. Three different formats of CO emissions from CARS, (A) District-level total emissions
1038   (t yr^{-1}) (B) Link-level total emissions (t yr^{-1}), (C) CTM-ready gridded hourly total emissions (moles
1039   s^{-1}).
1040
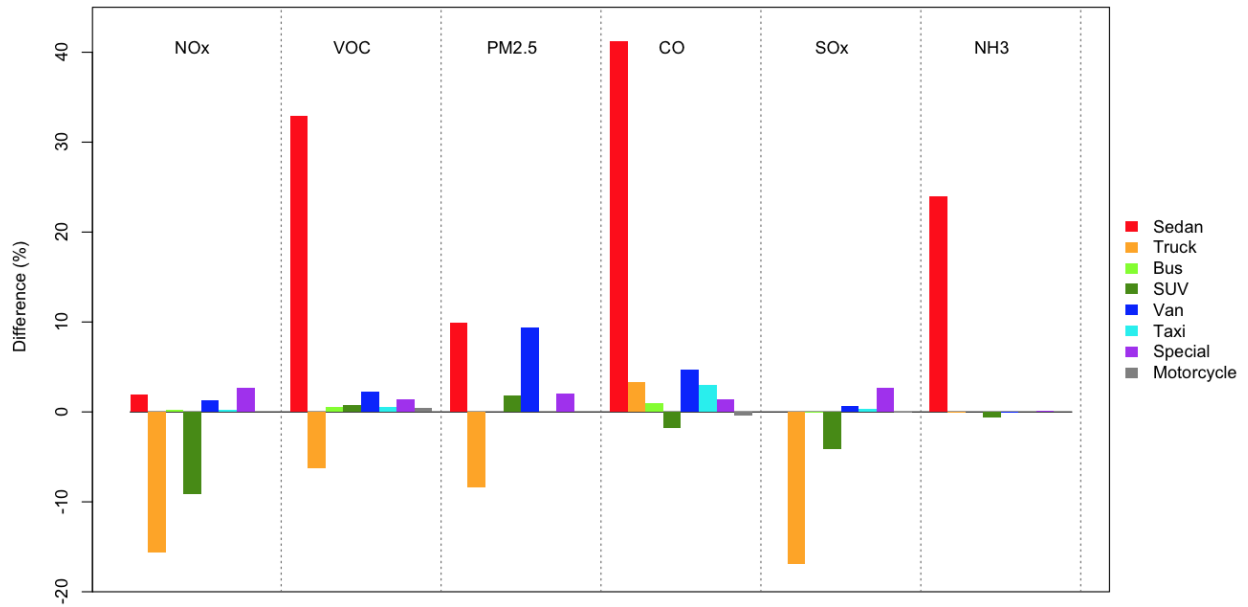
1041
1042 **Figure 8**. Comparison between CARS 2015 and CAPSS 2015 onroad mobile emissions
1043 inventories by vehicle types. The standard line is CAPSS 2015 data.
1044
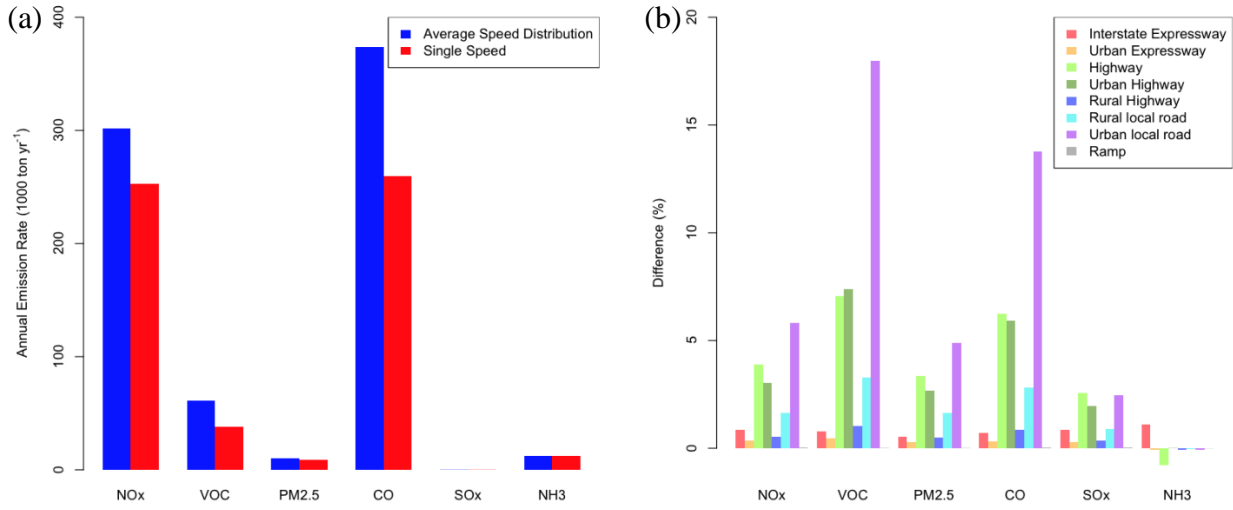
Figure 9. The impacts of emissions between the ASD and single-speed approach: (a) the total
emission differences by pollutant; (b) The road-specific difference (%) by pollutant.

1050   **Appendices**
1051

1052

1053   **Appendix A**: The vehicle types classified by fuel type, vehicle body type, and engine size. The
1054   emission factors of the diesel vehicle with the star (*) are depended on the ambient temperature
1055   (*T*).

Vehicle Types	Fuel Types							
	Gasoline	Diesel	LPG	CNG	HYBRID_G	HYBRID_D	HYBRID_L	HYBRID_C
Sedan	Supercompact	Supercompact*	Supercompact	-	-	-	-	-
	Compact	compact*	compact	compact	compact	compact	compact	-
	Fullsize	Fullsize*	Fullsize	Fullsize	Fullsize	Fullsize	Fullsize	-
	Midsize	Midsize*	Midsize	Midsize	Midsize	Midsize	Midsize	-
Truck	Supercompact	Supercompact	Supercompact	-	-	-	-	-
	Compact	Compact*	Compact	Compact	-	-	-	-
	Fullsize	Concrete	-	Fullsize	-	-	-	-
	Midsize	Fullsize	Midsize	Midsize	-	-	-	-
	-	Midsize	-	-	-	-	-	-
	-	Dump	-	-	-	-	-	-
	-	Special	Special	Special	-	-	-	-
Bus	Urban	Urban	Urban	Urban	-	Urban	-	-
	-	Rural	-	Rural	-	Rural	-	Rural
SUV	Compact	Compact*	Compact	-	-	-	-	-
	Midsize	Midsize*	Midsize	Midsize	Midsize	-	-	-
Van	supercompact	supercompact	supercompact	-	-	-	-	-
	Compact	Compact	Compact	Compact	-	-	-	-
	-	-	Fullsize	Fullsize	Fullsize	Fullsize	Fullsize	Fullsize
	Midsize	Midsize	Midsize	Midsize	Midsize	Midsize	Midsize	Midsize
Taxi	-	-	Compact	-	-	-	-	-
	-	-	Fullsize	-	-	-	-	-
	-	-	Midsize	-	-	-	-	-
Special	-	Tow	-	-	-	-	-	-
	Wrecking	Wrecking	Wrecking	Wrecking	-	-	-	-
	Others	Others	Others	-	-	-	-	-
Motorcycle	Compact	-	-	-	-	-	-	-
	Midsize	-	-	-	-	-	-	-
	Fullsize	-	-	-	-	-	-	-

1056   - no existence
1057   * ambient temperature-dependent diesel vehicle
1058   LPG: Liquefied Petroleum Gas
1059   CNG: Connecticut Natural Gas
1060   Hybrid_G: hybrid vehicle with gasoline
1061   Hybrid_D: hybrid vehicle with diesel
1062   Hybrid_L: hybrid vehicle with LPG
1063   Hybrid_C: hybrid vehicle with CNG

1064
1065

Appendix B, The summary of activity data (number of vehicles and daily total VKTs) in South
Korea by vehicle type with engine size.

Vehicle Types	Engine sizes	Fuel Types									
		Gasoline		Diesel		LPG		CNG		Hybrid	
		Numbers	Daily VKT	Numbers	Daily VKT	Numbers	Daily VKT	Numbers	Daily VKT	Numbers	Daily VKT
Sedan	Supercompact	1,792,471	50,197,345	46	1,761	83,226	4,000,067	6	237	-	-
	Compact	1,372,317	39,543,668	51,324	2,570,086	8,040	257,060	276	12,115	3,802	137,360
	Fullsize	2,403,327	100,632,702	428,831	20,928,552	292,850	15,910,588	5,296	323,852	21,533	1,086,509
	Midsize	4,858,533	167,454,032	672,960	33,126,318	1,431,970	66,640,378	4,310	625,717	140,527	6,717,856
Truck	Supercompact	850	9,595	816	354	111,051	6,550,476	-	-	-	-
	Compact	3,185	143,510	2,655,089	133,480,216	87,650	3,567,109	42	2,694	-	-
	Fullsize	3	422	180,991	25,774,819	-	-	72	4,676	-	-
	Midsize	98	7,430	258,509	17,477,685	1,434	47,870	14	483	-	-
	Dump	-	-	-	-	-	-	-	-	-	-
	Special	20	970	-	-	2,292	99,124	1,194	60,886	-	-
Bus	Urban	1	126	40,448	7,282,593	1	652	6,543	1,466,854	2	282
	Rural	-	-	34,997	6,334,278	-	-	30,792	6,460,001	216	50,873
SUV	Compact	42,348	1,395,153	2,341,397	105,962,626	6,946	275,728	13	551	-	-
	Midsize	91,002	3,520,552	1,120,128	5,277,861	13,567	595,426	15	706	1,719	88,683
Van	supercompact	88	1,645	-	-	44,947	2,058,014	-	-	-	-
	Compact	2,937	87,507	685,317	34,781,937	151,654	6,135,138	7	255	-	-
	Fullsize	-	-	19,452	1,318,221	1	14	97	7,598	3	136
	Midsize	2	1,303,795	31,790	1,433,407	15	416	160	15,216	2	85
	Special	-	-			-	-	-	-	-	-
Taxi	Compact	-	-	-	-	8,380	576,378	-	-	-	-
	Fullsize	-	-	-	-	92,861	10,827,756	-	-	-	-
	Midsize	-	-	-	-	474,455	69,087,721	-	-	-	-
Special	Tow	-	-	40,807	7,447,773	-	-	-	-	-	-
	Wrecking	2	138	12,568	813,746	128	6,607	3	94	-	-
	Others	47	553	28,275	989,988	180	9,966	-	-	-	-
Motorcycle	Compact	184,822	3,507,948	-	-	-	-	-	-	-	-
	Fullsize	65,964	3,493,728	-	-	-	-	-	-	-	-
	Midsize	1,910,988	61,676,824	-	-	-	-	-	-	-	-

1068 - no existence
1069 LPG: Liquefied Petroleum Gas
1070 CNG: Connecticut Natural Gas
1071 Hybrid: all hybrid vehicles, electric power mixed with fossil fuel (gasoline, diesel, LPG, or CNG)

1072

1073

1074

1075

1076 **Appendix C**, Eight road types with assigned average vehicle operating speed and VKT fractions.

Road types	Description	Average Speed (km h^{-1})	Road VKT fraction
101	Interstate Expressway	90	41%
102	Urban Expressway	60	5%
103	Highway	58	18%
104	Urban Highway	36	12%
105	Rural Highway	55	3%
106	Rural Local Road	45	4%
107	Urban Local Road	32	17%
108	Ramp	50	0.4%

1077
1078

1079 **Appendix D,** The daily average VKT (km d^{-1}) per vehicle by vehicle and fuel types.

Vehicle types	Fuel Types					
	Gasoline	Diesel	LPG	CNG	Hybrid	Average
Sedan	34	49	48	97	48	38
Truck	39	57	51	52	-	57
Bus	126	180	-	212	237	191
SUV	37	46	42	45	52	46
VAN	29	51	42	87	44	49
Taxi	-	-	140	-	-	140
Special	14	113	54	31	-	113
Motorcycle	32	-	-	-	-	32

1080

1081

Appendix E, Average speed distribution (ASD) for each road type: The table columns are different road types, and the table rows are average speed of each speed bin.

Speed bins	Speed (km/h)	Road Types							
		101	102	103	104	105	106	107	108
1	speed < 4	1.50%	2.00%	5.00%	5.00%	5.00%	10.00%	10.00%	0.00%
2	4 ≤ speed < 8	0.50%	1.00%	2.00%	2.00%	2.00%	5.00%	5.00%	0.00%
3	8 ≤ speed < 16	0.00%	0.33%	0.40%	3.59%	0.41%	0.30%	2.76%	0.11%
4	16 ≤ speed < 24	0.00%	1.09%	3.64%	14.35%	1.45%	2.91%	11.75%	5.85%
5	24 ≤ speed < 32	0.01%	3.04%	6.82%	35.25%	6.85%	6.15%	40.80%	12.80%
6	32 ≤ speed < 40	0.17%	6.43%	9.28%	17.14%	14.70%	12.00%	12.69%	24.53%
7	40 ≤ speed < 48	0.52%	14.76%	10.70%	10.86%	16.20%	23.30%	7.49%	23.74%
8	48 ≤ speed < 56	0.53%	16.66%	12.52%	5.72%	15.42%	20.72%	4.24%	6.60%
9	56 ≤ speed < 64	1.94%	23.49%	12.83%	2.68%	6.08%	10.06%	2.56%	10.90%
10	64 ≤ speed < 72	5.05%	16.30%	10.51%	1.90%	13.21%	3.84%	1.45%	5.30%
11	72 ≤ speed < 80	11.70%	10.19%	12.69%	0.74%	9.98%	2.85%	0.53%	5.30%
12	80 ≤ speed < 89	28.73%	4.30%	12.21%	1.04%	6.75%	2.21%	0.65%	4.59%
13	89 ≤ speed < 97	34.24%	0.51%	1.82%	0.15%	1.90%	0.62%	0.08%	0.00%
14	97 ≤ speed < 105	14.99%	0.00%	0.02%	0.00%	0.04%	0.03%	0.00%	0.30%
15	105 ≤ speed < 113	0.18%	0.00%	0.00%	0.00%	0.00%	0.00%	0.00%	0.00%
16	113 ≤ speed < 121	0.01%	0.00%	0.00%	0.00%	0.00%	0.00%	0.00%	0.00%

Appendix F: Single average speed for each road type

Speed bins	Speed (km/h)	Road Types							
		101	102	103	104	105	106	107	108
1	speed < 4	0%	0%	0%	0%	0%	0%	0%	0%
2	4 ≤ speed < 8	0%	0%	0%	0%	0%	0%	0%	0%
3	8 ≤ speed < 16	0%	0%	0%	0%	0%	0%	0%	0%
4	16 ≤ speed < 24	0%	0%	0%	0%	0%	0%	0%	0%
5	24 ≤ speed < 32	0%	0%	0%	0%	0%	0%	100%	0%
6	32 ≤ speed < 40	0%	0%	0%	100%	0%	0%	0%	0%
7	40 ≤ speed < 48	0%	0%	0%	0%	0%	100%	0%	100%
8	48 ≤ speed < 56	0%	0%	100%	0%	100%	0%	0%	0%
9	56 ≤ speed < 64	0%	100%	0%	0%	0%	0%	0%	0%
10	64 ≤ speed < 72	0%	0%	0%	0%	0%	0%	0%	0%
11	72 ≤ speed < 80	0%	0%	0%	0%	0%	0%	0%	0%
12	80 ≤ speed < 89	100%	0%	0%	0%	0%	0%	0%	0%
13	89 ≤ speed < 97	0%	0%	0%	0%	0%	0%	0%	0%
14	97 ≤ speed < 105	0%	0%	0%	0%	0%	0%	0%	0%
15	105 ≤ speed < 113	0%	0%	0%	0%	0%	0%	0%	0%
16	113 ≤ speed < 121	0%	0%	0%	0%	0%	0%	0%	0%

1086   **Appendix G**:

1087

1088   The annual emission rate between original road type ASD, adjusted road type ASD, and CAPSS
1089   result for 2015

Gg/year	CO	NOx	SOx	PM10	PM2.5	VOC	NH3
CARS data 2015 org ASD	269.3	258.4	0.2	9.5	8.8	38.9	12.4
CARS data 2015 adj ASD	373.9	301.8	0.2	11.0	10.1	61.2	12.5
CAPSS 2015	245.5	369.6	0.2	9.6	8.8	46.1	10.1

1090

1091

1092

1093   **Appendix H**:

1094

1095   CARS model input data summary table

Input data type	Parameters	Variable Name in CARS	File format
Human activity data of each vehicle	Fuel, vehicle, type, daily VKT, region code, manufacture data	activity_file	csv
Emission factor table	Vehicle, engine, fuel, SCC ,Pollutant, year, temperature, v,a,b,c,d,f,k	Emis_factor_list	csv
Link level Shape file	Link ID, region code, region name, road rank, speed, VKT, Link length, geometry	Link_shape	shape file
County Shape File	Region code, region name	county_shape	shape file
Average speed distribution table	Speed bins, the distribution of each road type	avg_SPD_Dist_file	csv
road restriction table	Vehicle, engine, fuel, road types	road_restriction	csv
Vehicle deterioration table	Vehicle, engine, SCC, fuel, Pollutant, Manufacture date	Deterioration_list	csv
Control strategy factors table	Vehicle, engine, fuel, year, data, region code, control factor	control_list	csv
Model domain description	Projection method name, parameters for prjection method, domain name, bottum left coner X and Y, grid cell size, numbers of grid cell in X, Y, and Z-axis	gridfile_name	text file in griddesc format
Temporal profile tables	Profile reference number, Year to Monthly profile (12 columns)	temporal _monthly_file	csv
	Profile reference number, week to daily profile (7 columns)	temporal _week_file	csv

	Profile reference number, week day to hourly profile (24 columns)	temporal_weekday_file	csv
	Profile reference number, weekend day to hourly profile (24 columns)	temporal_weekend_file	csv
	Vehicle, types, fuel, road type, month reference number, week reference number, weekday reference number, weekend reference number	temporal_CrossRef	csv
Chemical profile table	Species code, species name, target species name, fraction, molecular weight,	Chemical_profile	txt or csv
	Vehicle, engine, fuel, species reference codes	speciation_CrossRef	csv

1096
1097